AD NUMBER

ADB008182

LIMITATION CHANGES

TO:

Approved for public release; distribution is unlimited.

FROM:

Distribution authorized to U.S. Gov't. agencies only; Test and Evaluation; NOV 1974. Other requests shall be referred to Air Force Materials Laboratory, Attn: Nonmetallic Materials Division, Elastomers and Coastings Branch, AFML/MBE, Wright-Patterson AFB, OH 45433.

AUTHORITY

AFWAL Notice dtd 3 Nov 1983

AD B00 81 82

AUTHORITY:
AFWAL
Notice 3 Nov 83

AFML-TR-75-17

ML-101 THERMAL CONTROL COATING SPACEFLIGHT EXPERIMENT

ELASTOMERS AND COATINGS BRANCH
NONMETALLIC MATERIALS DIVISION

AUGUST 1975

TECHNICAL REPORT AFML-TR-75-17
FINAL REPORT FOR PERIOD JANUARY 1972 – JANUARY 1974

AIR FORCE MATERIALS LABORATORY
AIR FORCE WRIGHT AERONAUTICAL LABORATORIES
Air Force Systems Command
Wright-Patterson Air Force Base, Ohio 45433.

NOTICE

When Government drawings, specifications, or other data are used for any purpose other than in connection with a definitely related Government procurement operation, the United States Government thereby incurs no responsibility nor any obligation whatsoever; and the fact that the government may have formulated, furnished, or in any way supplied the said drawings, specifications, or other data, is not to be regarded by implication or otherwise as in any manner licensing the holder or any other person or corporation, or conveying any rights or permission to manufacture, use, or sell any patented invention that may in any way be related thereto.

This report was submitted by the Elastomers and Coatings Branch, Nonmetallic Materials Division, Air Force Materials Laboratory, Air Force Systems Command, Wright-Patterson Air Force Base, Ohio under job order 73400703. Daniel E. Prince (AFML/MBE) was the laboratory project engineer.

This technical report has been reviewed and is approved for publication.

Daniel E. Prince

Daniel E. Prince
Project Monitor

FOR THE COMMANDER

M. L. Minges

M. L. Minges
Chief, Elastomers and Coatings Branch
Nonmetallic Materials Division

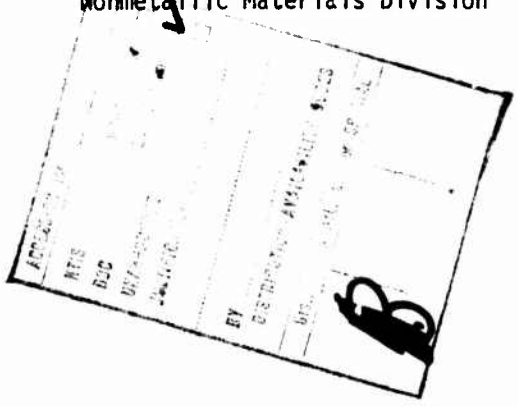

Copies of this report should not be returned unless return is required by security considerations, contractual obligations, or notice on a specific document.

AIR FORCE - 12-12-75 - 200

Block 20 (continued)

Based on selected data from over 5000 revolutions covering a period of one year, it was found that all the coatings initially degraded to a greater degree than expected, possibly due to contamination. The most stable coatings were optical solar reflectors and the least stable was a white α-Al_2O_3 pigmented coating. An experimental fabric material showed greater stability than state-of-the-art white coatings.

FOREWORD

This report was submitted by the Elastomers and Coatings Branch, Nonmetallic Materials Division, Air Force Materials Laboratory, Air Force Systems Command, Wright-Patterson Air Force Base, Ohio. The work was performed under Project 7340, Job Order 73400703. Daniel E. Prince (AFML/MBE) was the laboratory project engineer.

Contributions by Lt. M. Blessing, AFML/MBE, to data reduction and analysis were greatly appreciated.

TABLE OF CONTENTS

LIST OF ILLUSTRATIONS

LIST OF ILLUSTRATIONS (Continued)

LIST OF ILLUSTRATIONS (Concluded)

LIST OF TABLES

LIST OF SYMBOLS

SYMBOL	DESCRIPTION	UNITS
A_e	Area of edge of sample	ft^2
A_n	Cross-sectional area of sample	ft^2
C_p	Specific heat of sample	BTU/lbm-°R
F_{e-m}	Shape factor from edge of sample to Mylar holder	---
F_{e-s}	Shape factor from edge of sample to space	---
G	Solar heating constant	BTU/ft^2-hr
H_p	Incident planetary heating flux	BTU/ft^2-hr
H_r	Incident planetary albedo heating flux	BTU/ft^2-hr
H_s	Incident solar heating flux	BTU/ft^2-hr
I	Current	Amps
K	Thermal Conductance of sample	BTU/hr-°R
M	Mass of sample	lbm
Q_{ne}	Net heat exchange rate between sample and Mylar	BTU/hr
Q_{rs}	Total solar heat incident on sample edge	BTU/hr
T_s	Temperature of sample	°R
T_m	Temperature of adjacent Mylar	°R
T_n	Temperature of adjacent samples	°R
T_{ref}	Temperature of sample holder base	°R
α_s	Absorptance of sample	---
α_m	Absorptance of adjacent Mylar	---
ε_e	Emittance of sample edge	---
ε_{th}	Emittance of sample	---
ε_m	Emittance of Mylar holder	---
ε_n	Emittance of adjacent sample edges	---
σ	Stephan-Boltzmann constant, $0.17\ 14 \times 10^{-3}$	BTU/ft^2-°R^4

SECTION I
INTRODUCTION

The temperature control of spacecraft is one of the most challenging technical problems confronting spacecraft designers today. The ultimate objective of thermal design is to ensure that the spacecraft will operate within the prescribed temperature ranges defined by the temperature limitations of the spacecraft's materials and components, such as detectors, batteries, solar cells, and electronics, which operate properly and efficiently only if maintained within specific temperature ranges.

The surface temperature of a spacecraft depends primarily upon the solar radiation absorptance (α_s) of the surface, the radiation of solar energy from the surface or surface emittance (ε), and the generation of heat in the body of the spacecraft. Secondary parameters that influence the surface temperature of a spacecraft are material properties such as thermal conductivity and specific heat of components. Solar absorptance is defined as the ratio of solar energy absorbed by a surface to that absorbed by a blackbody, while emittance is the ratio of the energy radiated from a surface to that radiated from a blackbody at the same temperature.

Two techniques are used for regulating spacecraft temperatures: active systems and passive systems. Active systems usually employ electrical power and moving parts which can be adjusted providing a constantly varying surface in terms of optical properties. Passive systems, in contrast, require neither electrical power nor moving parts and rely on surfaces with appropriate thermophysical properties; namely, solar absorptance, α_s and infrared emittance (ε). Regardless of what combination of systems is used, the thermophysical properties of the entire spacecraft surface must be known since it is the average surface properties which determine the spacecraft equilibrium temperature.

Because of the large role surface coatings play in the passive temperature control of spacecraft, extensive programs have been conducted

to develop space-stable, low α_s/ε coatings. Future spacecraft requirements call for the development of coatings with an initial solar absorptance of less than 0.10 and initial emittance of more than 0.90, with long-term stability (5-10 years) in the space environment; i.e., increase in α_s of less than 10%. Low α_s/ε surfaces can be divided into three divisions: (1) those represented by diffusely reflecting white pigmented coatings, or paints; (2) those represented by second surface mirrors that obtain their low solar absorptance from the metallic reflection of an aluminum or silver mirror and their emittance from a selectively transmitting substrate such as quartz or FEP Teflon; and (3) those represented by newly emerging white fabric cloth materials.

Many of the previous materials have been extensively subjected to in situ laboratory simulation exposures, however, most important to the thermal designer is knowledge of actual spaceflight data and its correlation with laboratory data. This report describes an Air Force Materials Laboratory coatings spaceflight experiment whose primary objective was to determine the effects of the space environment on the equilibrium-radiative properties of selected candidate temperature control coating systems. Its secondary objective was to correlate the actual space degradation with simulated laboratory data.

SECTION II
SATELLITE ORBITAL PARAMETERS AND EXPERIMENTS

The Space Test Program (STP) is a Department of Defense program for the spaceflight of research and development payloads as well as operational payloads. The STP P72-1 flight vehicle was launched from Vandenberg Air Force Base on an Atlas-F/BII combination. Liftoff occurred at 2012.5 Z on 2 October 1972. The satellite orbit was sun-synchronous with a nominal inclination of 98.34 degrees (polar) and a nominal circular altitude of 400 nautical miles. The initial orbital parameters and the orbital parameters as of September 30, 1973 are compared to the planned nominal parameters for the 72-1 vehicle in Table I.

TABLE I
SATELLITE ORBITAL PARAMETERS

Flight Parameters	Planned Nominal	Actual (Initial)	Actual (Sep 1973)
Maximum altitude (nm)	409.19	411.41	411.21
Minimum altitude (nm)	398.13	400.37	399.27
Eccentricity	0.00041375	0.00039	0.00055995
Inclination (deg)	98.348	98.424	98.433
Period (min:sec)	99:40.158	99:39.465	99:39.217
Rev. No.		1	5191

The 72-1 satellite included a payload of six experiments. These are listed in Table II together with the type of experiment, principal investigator, and appropriate organization.

TABLE II
SATELLITE PAYLOADS

Experiment No.	Investigator & Organization	Description
ML-[illegible]1	D. E. Prince Air Force Materials Laboratory	Thermal Control Coatings
RTD-802	A. Y. Harper ABMDA-Huntsville	Radar calibration target
ARPA-501	J. B. Reagen Lockheed Research Laboratory	Gamma-spectrometer
NNRL-114	C. S. Weller Naval Research Laboratory	Extreme UV radiation
SSD-988A	D. R. Croley, Jr. Aerospace Corporation	Low altitude particles
SSD-988B	P. Rothwell AFCRL: Hanscom Field	Low altitude particles

SECTION III
STP FLIGHT P72-1 SATELLITE SYSTEMS

1. ELECTRICAL POWER SYSTEM

The satellite electrical power is supplied by a solar cell array that generates electrical energy required to operate the satellite subsystem and experiments and to charge two nickel-cadmium batteries that supply electrical power during solar eclipse. The electrical power is distributed directly from the main power bus or switched by a relay control box by uplink command.

2. TELEMETRY, TRACKING, AND COMMAND SYSTEM

The telemetry system transmits all data in PCM/PM at 8 or 64 Kbps real-time and recorded data at 64 or 512 Kbps. A 2-watt SGLS reference transmitter is used for the 8 Kbps rate and a 10-watt data transmitter is used for the 64 and 512 Kbps data rate. The processor furnishes multiplexing, analog to digital conversion (where required) formatting, clocking, and synchronizing signals for the TT&C systems including the programmer. Three tape recorders are supplied for reliability and high data capacity for unusually high peak load periods. All other systems are dual redundant. A command system which is also dual redundant, includes the Command Receiver Demodulator and the Decoder/Programmer which provides 375 MHz system real-time uplink command capability and stored program routines for flexible payload and telemetry system control.

3. STABILIZATION, ORIENTATION, AND ATTITUDE DETERMINATION

The STP P72-1 satellite operates in a sun-synchronous orbit with the spin axis nominally normal to the orbit plane within five degrees with a goal of one degree. The satellite spin speed is controlled within 12 ± 2 rpm.

The Satellite Attitude Control System (ACS), makes use of magnetic torque coils to control the attitude and spin rate of the highly stable spinning vehicle. Body fixed earth sensors provide data for primary

determination of attitude and rate. Ground commands control the torque coil current to provide correction of observed errors. Wobble damping is provided by a passive fluid loop damper.

Measurement of the earth's magnetic field is provided by two three-axis magnetometers mounted on the forward antenna boom. The associated Magnetometer Electronics Assembly provides proportional outputs that are multiplexed into the telemetry stream. The outputs are used as a polarity sense switch for spin control and provide data for the backup attitude and spin rate determination.

A dual winding iron-core precession coil is used to maintain the spin axis within five degrees of the orbit normal. The coil is operated continuously to provide orbit regression rate. Periodic updates by ground control commands to the multitap precession coil eliminate any buildup of errors caused by random disturbance torques or bias in the satellite magnetic field. Attitude information is provided by a redundant horizon sensor system. A spin rate control coil, identical to the precession coil, is provided to update the satellite spin speed on command from the ground. The coil is automatically commutated by radial magnetometer output signals. Backup capability is provided by cross strapping a backup magnetometer through the PCM Processors to the dual spin coil windings.

SECTION IV
EXPERIMENTAL PACKAGE

The complete basic design and initial evaluation data are contained in References 1 and 2. Sample holders used on the 72-1 satellite are Numbers 7 and 12. Each sample holder weighs approximately 11 ounces (300 grams), occupies approximately 40 cubic inches, and will accommodate five test samples and one reference sample. The samples or thermal control coating specimens are 15/16 inch in diameter with the thickness depending on coating applied and substrate. The sensor disks used for the sample holders are Trans-Sonics T4086-3 platinum resistance thermistors cemented in stainless steel sensor disks. Each platinum thermistor has been calibrated to an accuracy of $\pm 0.5^{\circ}C$ at temperatures of $-193^{\circ}C$, $0^{\circ}C$, and $100^{\circ}C$. The constants for the temperature resistance relationship of platinum are supplied with each sensor and are used in translating resistance to temperature. A sensor (Trans-Sonics T4086-3) is attached to the bottom surface of the holders as a temperature reference for correction of conduction losses from the sample sensors.

The sensors are supported upon 50 layers of super-insulation (1/4 mil Mylar aluminized on one side) by a continuous Dacron cord under tension. The individual samples and sensors are thus thermally isolated from each other with the primary conduction loss through the thin sensor leads. A temperature sensor is placed adjacent to the electrical connector to permit correction of flight data for this loss. Ten pounds of tension is placed on the Dacron thread used to bind the sensors in place during fabrication. Each sensor is held at three places by the cord and is cemented to the cord at these points. The sensors rest upon a three mil sheet of Mylar (aluminized side down) which acts as a cover for the Dacron cord.

The measurement of the resistance of the sensors is obtained by supplying an external voltage (90 millivolts) to the sensors and measuring the voltage drop across each sensor. The voltage drop across each thermistor is in turn a linear function of resistance which in turn is

a linear function of temperature for this range. Through the calibration data for each thermistor, the temperature can be determined. Room temperature calibration was performed in both real-time and tape recorder modes in the pre-launch satellite acceptance test phase. This calibration data obtained prior to launch together with the installed flight hardware is being used for the data reduction and then calculation of the desired thermophysical values.

Figure 1 shows the ML-101 sample holder with six coatings attached and Figure 2 shows the ML-101 sample holders attached to the partially completed 72-1 satellite.

SECTION V
EXPERIMENTAL THERMAL CONTROL COATINGS

A total of 12 thermal control coating samples were used on two sample holders for the ML-101 spaceflight thermal control coating experiment. The sample holders are designated 7 and 12 on all experiment references.

7-1, ZnO (Silicate Coated)/Methyl Silicone (S-13G)

Formulation, processing, and application was performed by IITRI* in accordance with IITRI Report 4-6053-5-7; Batch No. C-133. The S-13G was sprayed to a thickness of 8.0 + 1.0 mils.

7-2, SiO_2 Cloth Fabric

2024-T3 unclad 15/16 inch diameter 0.032 inch thick aluminum substrate was prepared as follows: (1) faced on 240 SiC stationary grinder, (2) prepolished with jeweler's rouge and buffed, and (3) final polished using Buehler's Magomet (M_gO) on Microcloth. The silica cloth fabric is a 12 harness double layer satin weave woven from 450/1/0 Suprasil yarn. Polyvinylalcohol sizing was removed by heating, and filament diameter size was six microns. The fabric construction consists of 150 ends/inch by 240 picks/inch. The fabric thickness is nominally 0.005 inch and weighs 4.65 oz/yd^2. The fabric was bonded to the polished aluminum substrate with General Electric SR-585 silicone adhesive and the entire system vacuum outgassed at 375°F.

7-3, Aluminized 5 mil FEP Teflon Second Surface Mirror

This material was manufactured by G. T. Schjeldahl, Northfield, Minnesota, Type G400900, lot number 12-33 and was supplied to the AFML through the courtesy of Mr. A. E. Hultquist, Lockheed Missiles and Space Company of Sunnyvale, California. The material was bonded to a 15/16 inch diameter 2024 NaOH etched aluminum disc in the following manner. Both the front side of the disc and the back side of the vacuum

* ITT Research Institute, Technology Center, Chicago, Illinois.

deposited aluminum were primed with General Electric SS4004 clear silicone primer and then 3M Company's Number 465 adhesive transfer tape was used on both the disc and the back side of the vacuum deposited aluminum layer and pressure applied by hand rubbing with 0.125 inch Teflon sheet.

7-4, Zn_2TiO_4/Methyl Silicone

Pigment synthesis, coating formulation, and application was performed by the Illinois Institute of Technology using Owens Illinois 650 methyl silicone resin as a binder material. Coating thickness was 5 $\pm$ 1.0 mils.

7-5, PV-100

This material is a rutile TiO_2 pigment in a silicone-alkyd binder, better known as Vita-Var heat absorption paint, formulation PV-100, 15966 white. The coating was prepared on 0.040 inch thick, 15/16 inch diameter 2024 aluminum disks after they were cleaned by solvent wiping followed with a sodium hydroxide etch and water rinse. Strontium chromate primer was applied per MIL-P-23377B to a thickness of 0.0005 inch. The PV-100 topcoat was then sprayed to a thickness of 0.002 inch and air-dried.

7-6, 3M Black Velvet

This is a two component polyester-epoxy paint, type 401-C10 prepared by dispersing three parts of Part A, Lot No. VC-39-125 and one part of Part B, Lot No. 16. This was then spray applied onto 0.032 inch aluminum discs which had been sanded, solvent wiped, and primed with G. E.'s SS4044 primer (thickness less than 0.001 inch). Thickness of the coating was 0.006 $\pm$ 0.001 inch.

12-1, TiO_2/Methyl Silicone

This coating consisted of a TiO_2 pigment (Dupont R-992, Lot No. 9980) in purified RTV 602 (G1638-46 EFG from Hughes Aircraft Company under Contract F33615-71-C-1155) polydimethylsiloxane A pigment to binder ratio of 150/100 was used. Thickness was 5.5 $\pm$ 0.5 mils.

12-2, Optical Solar Reflector, 0.008

This is a second surface mirror with the front surface consisting of 0.008 inch of Corning 7940 quartz, and the back surface coated with vacuum deposited silver, overcoated with Inconel and a final dielectric back cover. These samples were supplied to AFML through the cooperation of Mr. E. N. Borson, Aerospace Corporation and Mr. A. E. Hultquist, Lockheed Missile and Space Company. This material was bonded to the aluminum disc using the same procedure as sample 7-3.

12-3, Optical Solar Reflector 0.050

Same material as 12-2 except the Corning 7940 quartz was 0.050 inch thick. The same bonding procedure used on sample 7-3 was utilized.

12-4, Eu_2O_3/Methyl Silicone

This coating consisted of a europium oxide pigment (American Potash and Chemical, Code 1014, Lot No. D1031, silicate treated) in purified RTV 602 (G1638-46EFG from Hughes Aircraft under Contract F33615-71-C-1155) polydimethylsiloxane. A pigment to binder ratio of 270/100 was used. Thickness was 8.0 $\pm$ 1.0 mils.

12-5, αAl_2O_3/Methyl Silicone

This coating was made from an α-alumina pigment (#1013 from Martin-Marietta Company under Contract F33615-71-C-1410) in unpurified commercial RTV 602, Lot #242, polydimethylsiloxane. A pigment to binder ratio of 200/100 was used. Coating thickness was 8.0 $\pm$ 1.0 mils.

12-6, 3M Black

A duplicate 3M Black per sample 7-6.

7-7 and 12-7 Reference Temperatures

Junction inside each sample holder.

54-6 Calibrated Resistor

A 499 ohm resistor in sample holder number 7, used as a check on voltage variations.

SECTION VI
OPTICAL PROPERTY DETERMINATION AND ENVIRONMENTAL EXPOSURE

Table III provides initial data for each coating, including mass, emittance, solar absorptance, and specific heat. The solar absorptance (α_s) value for each coating was determined utilizing a Beckman DK-2A spectrophotometer with a Gier-Dunkle Integrating Sphere and a xenon energy source (Figure 3). Integration of solar absorptance was accomplished using 25 points in conjunction with F. S. Johnson Solar Spectrum. In-air infrared spectral reflectance of each coating was measured in-house utilizing a Gier-Dunkle Model DB100 Portable Infrared Reflectometer (Figure 4). Subtracting the infrared reflectance from unity gave the total normal emittance. The theory employed by this instrument has been described by Nelson, et al (Reference 3).

Figure 5 depicts the AFML In Situ Exposure Device for simulation of ultraviolet-vacuum space conditions. The system was operated generally in the 10^{-7} torr region during radiation exposure. A xenon lamp ultraviolet source was used with an ultraviolet sun rate of approximately 1.25. The coating reflectance values were measured in situ before and after ultraviolet radiation exposure utilizing a Beckman DK-2A spectrophotometer with an integrating sphere inside the exposure chamber. Figures 6 through 15 present typical reflectance curves, before and after 500 EUVSH, for the coating samples flown. The pre-test and post-test solar absorptance values are also given for each coating.

TABLE III
INITIAL DATA INPUTS

Coating	Holder No.	Mass (lb_m)	ϵ_N	Initial Solar Absorptance	Specific Heat
S-13G	7-1	0.0119	0.89	0.20	0.15
Silica Fabric	7-2	0.0109	0.85	0.25	0.15
FEP/Al	7-3	0.0117	0.80	0.14	0.15
Zn_2TiO_4/OI 650	7-4	0.0115	0.87	0.17	0.15
PV-100	7-5	0.0114	0.85	0.23	0.15
3M Black	7-6	0.0107	0.92	0.985	0.17
Reference	7-7	N/A	N/A	N/A	N/A
TiO_2/M-Silicone	12-1	0.0109	0.87	0.19	0.15
OSR (0.008)	12-2	0.0114	0.80	0.073	0.15
OSR (0.050)	12-3	0.0137	0.81	0.075	0.15
Eu_2O_3/M-Silicone	12-4	0.0110	0.92	0.13	0.15
α-Al_2O_3/M-Silicone	12-5	0.0110	0.90	0.11	0.15
3M Black	12-6	0.0107	0.92	0.985	0.17
Reference	12-7	N/A	N/A	N/A	N/A
Calibrated Resistor	54-6	N/A	N/A	N/A	N/A

SECTION VII
COMPUTER DATA ANALYSIS

1. HEAT BALANCE EQUATIONS

The heat balance equations, using the list of symbols, for a single sample of a thermal control coating on this experiment are:

$$Q\ (\text{input}) = Q\ (\text{direct solar}) + Q\ (\text{conduction}) \quad (1)$$

$$+Q\ (\text{sensor dissipation}) + Q\ (\text{reflected solar})$$

$$+Q\ (\text{albedo}) + Q\ (\text{earth emission})$$

$$Q\ (\text{output}) = Q\ (\text{emitted}) + Q\ (\text{exchange with surroundings}) \quad (2)$$

$$+Q\ (\text{storage})$$

The individual terms of Equations 1 and 2 are:

$$Q\ (\text{direct solar}) = \alpha_s A_n H_s \quad (3)$$

$$Q\ (\text{conduction}) = K(T_s - T_{ref}) \quad (4)$$

$$Q\ (\text{sensor dissipation}) = I^2R \text{ loss in sensor} \quad (5)$$

$$Q\ (\text{reflected solar}) = \text{reflected sunlight from the Mylar upper surface and other areas of surroundings} = Q_{rs} \quad (6)$$

$$Q\ (\text{albedo}) = \alpha_s A_n H_r \quad (7)$$

$$Q\ (\text{earth emission}) = \varepsilon_{th} A_n H_p \quad (8)$$

$$Q\ (\text{emitted}) = \varepsilon_{th} A_n \sigma T_s^4 \quad (9)$$

$$Q\ (\text{exchange with surrounds})$$

$$Q_{(nc)} = A_e \epsilon_e F_{e-s} \sigma T_s^4 + A_e F_{e-m} \sigma \epsilon_e \epsilon_m (T_s^4 - T_m^4) \quad (10)$$

$$+ \Sigma A_e F_{e-m} \sigma \epsilon_e \epsilon_n (T_s^4 - T_n^4)$$

$$Q\ (\text{storage}) = MC_p dT_s/d\theta \quad (11)$$

Combining Equations 1 - 11 results in:

$$\alpha_s A_n H_s + K(T_s - T_{ref}) + Q_{rs} + \alpha_s A_n H_r + \epsilon_{th} A_n H_p = \epsilon_{th} A_n \sigma T_s^4 + A_e \epsilon_e F_{e-s} \sigma T_s^4 + A_e F_{e-m} \sigma \epsilon_e \epsilon_m (T_s^4 - T_m^4) \tag{12}$$

where I^2R and $\Sigma A_e F_{e-m} \sigma \epsilon_e \epsilon_n (T_s^4 - T_n^4)$ are considered negligible terms. Letting $T_m = \left\{ \left[\alpha_m (H_s + H_r)/\epsilon_m + H_p \right] / \sigma \right\}^{1/4}$ and solving for $MC_p \frac{dT_s}{d\theta}$ results in the following:

$$MC_p \frac{dT_s}{d\theta} = A_n (H_s + H_r)\alpha_s + A_e F_{e-m} \epsilon_e \alpha_m (H_s + H_r) + (A_e F_{e-m} \epsilon_e \epsilon_m + A_n \epsilon_{th}) H_p + Q_{rs} + KT_{ref} - \sigma (A_n \epsilon_{th} + A_e F_{e-m} \epsilon_e \epsilon_m + A_e \epsilon_e F_{e-s}) T_s^4 - KT_s \tag{13}$$

Dividing by MC_p and defining the following:

$$AA = \frac{A_n (H_s + H_r)\alpha_s + A_e F_{e-m} \epsilon_e \alpha_m (H_s + H_r)}{MC_p} + \frac{A_e F_{e-m} \epsilon_e \epsilon_m H_p + KT_{ref} + Q_{rs} + H_p A_n \epsilon_{th}}{MC_p} \tag{14}$$

$$BB = \frac{K}{MC_p} \tag{15}$$

$$CC = \frac{\sigma (A_n \epsilon_{th} + A_e F_{e-m} \epsilon_e \epsilon_m + A_e \epsilon_e F_{e-s})}{MC_p} \tag{16}$$

upon substitution into Equation 13 gives:

$$\frac{dT_s}{d\theta} = AA - BBT_s - CCT_s^4 \tag{17}$$

From Equation 15, it can be seen that BB is a constant dependent only upon property factors. Likewise CC in Equation 16 is dependent upon the property factor of the particular sample in question. The term AA in Equation 14 contains the heat inputs, property factors, and the solar absorptance term which is the quantity to be calculated.

The resulting differential equation (Equation 17) cannot be solved analytically because it is nonlinear due to the T_s^4 term. It can be solved by La Place transform methods after the fourth order T_s^4 term is linearized by an expansion such as the Taylor series expansion with higher order terms being neglected. However, errors result by neglecting these higher order terms.

Another more accurate method is to use the Runge-Kutta integration technique with the aid of the computer which is the method chosen and explained in Section 2.

2. RUNGE-KUTTA INTEGRATION TECHNIQUE AND COMPUTER PROGRAM MB4

The fourth order Runge-Kutta integration method solves the differential equation (Equation 17) by giving a solution set of values of the dependent variable, T_s, for several increments of the independent variable, θ.

The method uses a variable step integration with the interval of integration being specified. An interval of 0.001 was used in this analysis. This varible step integration is designed to keep the maximum local relative error of the dependent variable less than 1×10^{-6}. The method integrates from one point to another. The initial point is assumed to be at $\theta = 0$ for the independent variable while the dependent value of temperature at $\theta = 0$ is given as T_{so}.

A program to solve the differential equation of the form of Equation 17 using Runge-Kutta integration techniques was written and appears in Appendix I. The program integrates from some initial condition (temperature T_{so} at time T zero) to some final condition

(temperature T_{sck} at time T check). The program then checks to see if the temperature found from the integration is the same as that given from telemetry readings to within 0.1°R. If the temperature does not agree the parameter AA is then adjusted by 1.0 unit until the temperature agrees. This adjustment of AA by 1.0 unit was found to be the best factor to use. Should the function begin to oscillate the agreement interval is increased to 0.4°R and AA adjusted until that interval of agreement is met.

After the integration is completed and the equation fit to match that received from telemetry data. the values of AA (fit parameter) and corresponding values of temperature calculated from integration and compared to T_{sck} are printed out. The solution set of temperatures found for the fitted differential equation from time zero to some later time is printed out. Then these can be checked against further points from telemetry for a good overall fit if desired.

The portion of the T_s versus θ telemetry curve that is fit, is the initial portion where the effect of H_r should be minimized and the points chosen for the fit should be the same for all the curves in which the α_s are to be compared. The portion of the curve used in this analysis begins with time zero and temperature T_{so} at 0.155 hours into the orbit after just passing into the sun. The final point for which the curve is fit is at time 0.47 hours later or 0.625 hours into the orbit. The temperature T_{sck} is the temperature from the T_s versus θ curve which occurs at this time and is used as a check temperature for fitting the differential equation solution to the telemetry curve. Although this relatively large interval allows more time for the effect of changing H_r to enter the system, it permits more smoothing of integrated data.

The reason the initial point of 0.155 hours into the orbit was chosen was that some of the telemetry curves to be compared did not have telemetry data until that time in the orbit. This is due to tracking acquisition that occurred on certain revolutions.

During the actual calculation, values of initial temperature T_{so} and check temperature T_{sck} for each sample for a given revolution are obtained. These are supplied to the program in the following order: Sample 7-6, 7-1, 7-2, 7-3, 7-4, 7-5, 12-1, 12-2, 12-3, 12-4, and 12-5.

The program then uses the data from the black sample 7-6 to fit the integrated equation to the telemetry data and obtain the amount of heat incident upon each of the samples. This is done by calculating the amount of heat from the equation for a fixed alpha (0.985). This can be done because the solar absorptance of the black samples should not change appreciably with exposure time. This amount of total heat input is then used to calculate the alphas for each of the nonblack samples after they are fit to their corresponding telemetry curves. The alpha values are then printed out along with coating property information used in the calculations.

3. ASSUMPTIONS

(a) The heat capacity, C_p, was assumed to be constant and the values given in Table III were used as the correct values for each sample.

(b) The value of the total solar heat incident on the sample edge, Q_{rs}, was constant at 0.0375 BTU/hr.

(c) The shape factor from the edge of the sample to Mylar holder, F_{e-m}, and the shape factor from edge of sample to space, F_{e-s}, were constant at 0.5.

(d) The planetary heating flux, H_p, was 18.1 BTU/hr-ft^2.

(e) The solar heating flux, H_s, and the planetary albedo heating flux, H_r, were constant and found from sample 7-6 for each revolution.

(f) The constant H_r assumption is made because only the initial portion of the temperature vs time curve is used where increasing H_r should have the smallest effect.

(g) The term $\Sigma A_e F_{e-m} \sigma \epsilon_e \epsilon_n (T_s^4 - T_m^4)$ is zero, indicating neglibible interaction between adjacent sample edges.

(h) Sensor dissipation or I^2R loss of the platinum resistors is taken as zero since the term at 500 ohms and 100 mv results in a temperature rise of about 1/4°F, which is well within our temperature error limits.

4. DEVELOPMENT OF TIME-TEMPERATURE PROFILES

The computer program presented in Appendix II was utilized to convert raw digital data tapes for each required revolution directly into time-temperature curves. The program utilizes ground based sensor calibration data and sample holder conduction coefficients to convert millivolts to resistance to temperature. The program also plots directly the reference temperature and the resistance of the reference calibrated resistor. Typical plots for all sensors are presented in Figures 16 through 28.

SECTION VIII
DISCUSSION OF RESULTS

Table IV presents the solar absorptance changes for the coatings investigated. Column one indicates the initial laboratory measured solar absorptance, column two the initial in space calculated solar absorptance (calculated during revolution number 46 after the satellite had stabilized), and column three the calculated in space solar absorptance after one year (5191 revolutions, 2160 EUVSH).

One of the most important features to be noted in Table IV is that the initial in space solar absorptances of the two OSR's are twice those measured in the laboratory. This indicates some form of contamination on the surfaces. This contamination, from all indications, was present even during revolution number one, indicating contamination during liftoff as well as contamination during the initial revolutions from outgassing of volatile constituents from the satellite materials.

The effects of contamination on the initial in space solar absorptance values for the other coatings appear much smaller with the greatest change being for FEP/Al. The OSR coatings and the FEP/Al coating were, undoubtedly, affected the most because of their low initial solar absorptance which produced low surface temperatures, therefore attracting condensable contaminants. Also their low initial solar absorptance values were the most vulnerable to changes caused by small amounts of contaminant. The two coatings, Eu_2O_3/m-silicone and α-Al_2O_3/m-silicone both had initial in space solar absorptances which were lower than those measured in the laboratory. The reasons for this are not clear, but these initial calculated values were used for determining the total solar absorptance changes in Figures 37 and 38.

Figures 29 through 38 present a comparison of laboratory simulated data and flight data for all the coatings flown, except for 3M black velvet. These figures also indicate the rate of change in solar absorptance over the one year exposure period. The flight $\Delta \alpha_s$

in these figures is the change in coating solar absorptance when compared to the initial calculated in space solar absorptance, not the initial laboratory values. For example, although the OSR(0.008) increased by 0.087 from laboratory to initial in space, it only increased another 0.025 after one year exposure in space and this is the $\Delta \alpha_s$ reported.

Each flight curve represents the compilation and analysis of 200 revolutions of data between revolution 1 and revolution 5191. The data scatter was extremely small, primarily because of the satellite stability in space and the large amount of data received per unit time (in this experiment each sample was pulsed every 0.9 seconds), which allowed for excellent computer data averaging. The actual plots of time-temperature curves from the raw data tapes showed minimal data scatter and maximum consistency from one revolution to the next. Over 800 data tapes were received during the first year which allowed for the selection of revolutions of primary interest.

From Figures 29 through 38 it can be seen that, in all instances, after 500 hours, the flight coatings were degrading more rapidly than the laboratory tested coatings. As indicated earlier, this can best be explained by the synergistic effect of contamination. If, as it appears, all surfaces were contaminated, the degradation of the coatings consisted of a combination of coating solar degradation plus solar degradation of the contaminant on the coating surface. Results from the Air Force Materials Laboratory D024 thermal control coatings experiment aboard SKYLAB, where samples were returned to earth from space and evaluated, clearly indicated the detrimental effects of contamination on thermal control coating stability. In all instances where contamination occurred during the SKYLAB exposure, solar degradation of the coatings increased much more rapidly than expected from laboratory tests.

Figures 30, 31, 35, 36, and 37 for SiO_2 Fabric, FEP/Al, two OSR's and Eu_2O_3, all indicate an initial solar absorptance increase during the early revolutions with a gradual leveling of degradation with continued exposure. This result indicates a trend toward saturation of degradation

for these coatings, however, additional data collection beyond one year is needed to confirm this as well as determine the degradation saturation point for all of the coatings.

One further note relative to the figures is that in Figure 38 the ordinate has been increased, because the degradation of the α-Al_2O_3 coating was much more severe than any other coating.

TABLE IV

INITIAL VS SPACE SOLAR ABSORPTANCE

Coating	Initial Laboratory Solar Absorptance	Initial In Space Solar Absorptance	In Space Solar Absorptance (one year)
S-13G	0.20	0.19	0.33
Silica Fabric	0.25	0.27	0.35
FEP/Al	0.14	0.18	0.22
Zn_2TiO_4/OI650	0.17	0.19	0.33
PV-100	0.23	0.27	0.42
TiO_2/M-Silicone	0.19	0.19	0.33
OSR (0.008)	0.073	0.16	0.185
OSR (0.050)	0.075	0.16	0.195
Eu_2O_3/M-Silicone	0.13	0.08	0.16
α-Al_2O_3/M-Silicone	0.11	0.08	0.28

SECTION IX
CONCLUSIONS AND RECOMMENDATIONS

1. CONCLUSIONS

a. Some form of contamination, most likely from outgassing materials from the satellite, caused flight degradation of the thermal control coatings to be more severe than ground simulated degradation.

b. Of all the coatings flown, the Optical Solar Reflectors (OSR's) were the most stable. No significant difference in degradation was observed for the two OSR's of different thicknesses. This would indicate that the solar degradation was primarily a surface phenomenon rather than a bulk phenomenon.

c. FEP/Al was very stable with a $\Delta\alpha_s$ = 0.04 after one year at 400 nautical miles (EUVSH $\tilde{=}$ 2,160 hrs).

d. Of the white coatings flown, Eu_2O_3/m-silicone was the most stable ($\Delta\alpha_s$ = 0.08) and Al_2O_3/m-silicone was the most unstable ($\Delta\alpha_s$ = 0.20).

e. The silica fabric material flown was more stable than the white coatings with a $\Delta\alpha_s$ of 0.08 after one year exposure.

2. RECOMMENDATIONS

a. This data could also be used to calculate changes in coating emittance. This was not done due to time limitations.

b. Additional thermal control coating experiments should be flown at or near synchronous orbit to more closely simulate the environment of operational Air Force satellites.

c. The STP 72-1 satellite has continued to function satisfactorily even after one year of orbit life. Data from the ML-101 experiment should continue to be analyzed to determine the effects of long-term space exposure on these thermal control coatings.

d. Correlation of the ML-101 degradation data with data obtained from the AFML D024 experiment aboard the manned SKYLAB orbital workshop should be attempted.

REFERENCES

1. RTD-TDR-63-4269, Design and Construction of Sample Holders for Orbital Temperature Control Coatings Experiment, Vol. 1, Design, Analysis, and Test Results, TRW Systems, April 1964.

2. RTD-TDR-63-4269, Calibration Data and Drawings, Vol. 2, TRW Systems, April 1964.

3. K. E. Nelson, E. E. Luedke, and J. T. Bevans, Journal of Spacecraft Rockets, Vol. 3, No. 5, p. 758, 1966.

APPENDIX I
COMPUTER PROGRAM MB4

XP( )	=	Theta printout and storage array.
YP( )	=	TS(1) printout and storage array.
TS (1)	=	Temperature of sample at time theta.
P (1)	=	Highest derivative value.
ACHECK ( )	=	Storage array for AA values.
TSCHEK ( )	=	Storage array for TS (1) values calculated and compared to TSCK.
AA	=	Constant in differential equation which is changed to fit different equation solution to telemetry curve in $(\frac{dTs}{d\theta} = AA - BBTs - CCTs^4)$.
BB, CC	=	Other differential equation constants.
NSC	=	Sample identifier label check for sample 7-6.
TCHECK	=	Time value at which differential equation solution check is to be made with curve from telemetry data.
REV	=	Revolution number.
TREF	=	Reference sample temperature.
G	=	Solar heating constant.
NEXEC	=	Counter of number of times calculation loop is executed.
NS	=	Sample identifier label.
XMASS	=	Mass of sample.
CP	=	Heat capacity of sample.
ES	=	Emittance of sample.
TSO	=	Initial value of temperature of sample for integration.
TSCK	=	Temperature at which check is to be made of integrated equation temperature with telemetry data value.
AS	=	Solar absorptance.
HS	=	Solar heat input.
HR	=	Earth albedo heat input.
HP	=	Planetary heat from earth.

TIMEE	=	Upper limit on time for integration.
QRS	=	Total solar heat incident on sample edge.
AN	=	Cross-sectional area of sample.
AE	=	Area of edge of sample.
FES	=	Shape factor edge sample to space.
FEM	=	Shape factor edge sample to Mylar.
EE	=	Emittance of edge of sample.
AM	=	Absorptance of adjacent Mylar.
EM	=	Emittance of Mylar holder.
ZK	=	Thermal conductance of sample.
SIG	=	Stephan-Boltzmann constant.
N	=	Order of equation to be integrated.
ICHECK	=	Check variable for oscillation of function, if oscil ting, agreement interval increased to 0.4°F.
THETA	=	Time.
DTHETA	=	Increment for integration.
NCOUNT	=	Counter.
NCT	=	Counter for printing out every 10th integration solution point.
NPLT	=	Counter of number of solution points.
SUBROUTINE F(THETA, TS, P)	=	Function subroutine for differential equation.
RKDF	=	Runge-Kutta subroutine.
IER	=	Error flag.

```
      PROGRAM RUNG(INPUT,OUTPUT)
C   PROGRAM SOLVES DIFFERENTIAL  EQUATION BY RUNGE KUTTA INTEGRATION
      DIMENSION XP(200),YP(200)
      DIMENSION TS(1),P(1)
      DIMENSION ACHECK(100),TSCHEK(100)
      COMMON AA,BB,CC
C
      DATA NSC/4H 7-6/
C   CHANGE THE FOLLOWING 3 CARDS FOR EACH RUNNING OF PROGRAM
      DATA TCHECK/.47/,REV/12900./
      DATA TREF/502./
      DATA G/450./
C
      DO 8436 NEXEC =1,11
      READ 8500,NS,XMASS,CP,ES
8500  FORMAT(T17,A4,T28,F5.4,T38,F3.2,T46,F3.2)
      IF(NS.EQ.NSC) GO TO 8660
      READ 8501,TSO,TSCK,AS
8501  FORMAT(T16,F4.0,T27,F4.0,T36,F2.1)
      GO TO 8661
8660  READ 8505,TSO,TSCK,AS
8505  FORMAT(T16,F4.0,T27,F4.0,T36,F4.3)
8661  HS=.318*G
      HR=.101*G
      HP=18.1
C
      TIMEE=.60
      QRS=.0375
C
      AN=.0048
      AE=.0011
      FEM=.5
      FES=FEM
      EE=.85
      AH=.34
      EM=.76
      ZK=6.E-05
      SIG=1.714E-09
      AA=(AN*AS*(HS+HR)+AE*FEM*EE*AH*(HS+HR)+AE*FEM*EE*EM*HP+ZK*TREF
     1 +QRS+HP*AN*ES)/(XMASS*CP)
C  OVERTUE THE STARTING VALUE OF AA
      BB=ZK/(XMASS*CP)
      CC=SIG*(AN*ES+AE*FEM*EE*EM+AE*EE*FES)/(XMASS*CP)
      N=1
      ITEST=0
      NCOUNT=0
      DELTS=0.1
      DELTS2=0.4
      ICHECK=0
130   THETA=0.
      TS(1)=TSO
      IF(ITEST.EQ.0.) GO TO 46
      PRINT 199
199   FORMAT(1H1,10X,*THETA*,14X,*TS*)
      THETA=0.
      TS(1)=TSO
46    DTHETA=.001
```

```
      NCT=0
      NPLT=1
60    CALL F(THETA,TS,P)
10    CALL RKDF(THETA,TS,N,DTHETA,IER)
      NCT=NCT+1
      IF(ITEST.EQ.1) GO TO 111
      IF(THETA.GE.TCHECK) GO TO 110
65    GO TO 60
110   DIF=(TS(1)-TSCK)
      IF(ABS(DIF).LE.DELTS) GO TO 120
      NCOUNT=NCOUNT+1
      IF(DIF)96,97,97
70    96  AA=AA+1.
      IF(ICHECK.EQ.2) DELTS=DELTS2
      ICHECK=1
      ACHECK(NCOUNT)=AA
      TSCHEK(NCOUNT)=TS(1)
75    GO TO 130
      97  AA=AA-1.
      IF(ICHEGK.EQ.1) DELTS=DELTS2
      ICHEGK=2
      ACHECK(NCOUNT)=AA
80    TSCHEK(NCOUNT)=TS(1)
      GO TO 130
      120 ITEST=1
      GO TO 130
      111 IF(NCT.LT.10) GO TO 60
85    XP(NPLT)=THETA
      YP(NLPT)=TS(1)
      NPLT=NPLT+1
      NCT=0
      60  IF(THETA.LE.TIMEE) GO TO 10
90    NPLT=NPLT-1
      PRINT 112,(ACHECK(L),TSCHEK(L),L=1,NCOUNT)
      112 FORMAT(2X,*AA=*,1PE11.4,2X,*TS=*,1PE11.6,2X,*AA=*,1PE11.4,2X,
     1  *TS=*,1PE11.4,2X,*AA=*,1PE11.4,2X,*TS=*,1PE11.4)
      PRINT 12,(XP(L),YP(L),L=1,NLPT)
95    12  FORMAT(2X,1P8E11.4)
      PRINT 1640,NPLT,NCOUNT,AA
      1640 FORMAT(10X,*NPLT=*,I4,*;NCOUNT = *,I5,*; AA = *,1PE11.4)
      PRINT 893,ITEST
      893 FORMAT(2X,*ITEST = *,IC)
100   PRINT 7901,REV,G,HS,HR,HP,TSC,TSCK
      7901 FORMAT(///,10X,*FOR REVOLUTION#*,F6.0,/,5X,*G=*,1PE11.4,2X,*HS=*,
     1PE11.4,2X,*HR=*,1PE11.4,2X,*HP=*,1PE11.4,2X,*TSO=*,1PE11.4,2X,*TSCK=*,1PE
     2CK=*,1PE11.4///)
      IF(NS.EQ.NSC) GO TO 1113
105   AS=(XMASS*CP*AA-ZK*TREF-QRS-(AE*FEH*EE*EH+AN*ES)*HP)/(AN*(HR+HS))
     1    -AE*FEH*EE*AH/AN
      PRIN  7900,NS,XMASS,CP,ES,BB,CC,AA,AS
      7900 FORMAT(2X,*FOR SAMPLE#*,A4,/,4X,*MASS = *,F6.4,2X,*CP = *,F4.2,
     1 2X,*ES = *,F4.2,/,6X,*BB = *,1PE11.4,2X,*CC = *,1PE11.4,2X,
110  2 *AA = *,1PE11.4,2X,*AS = *,1PE11.4,///)
      GO TO 8436
      1113 G=(XMASS*CP*AA-(AE*FEH*EE*EH+AN*ES)*HP-ZK*TREF-QRS)/(.419*(AN*AS+A
     1E*FEH*EE*AH))
      HS=.318*G
```

```
      PROGRAM RUNG        74/74   OPT=0   TRACE OEBUG              FTN 4.2+P380       05/20/75  10.31.43.       PAGE     4

  115                 HR=.101*G
                      PRINT 1114,G,HS,HR,HP
                1114  FORMAT(2X,*G=*,F4.0,2X,*HS=*,F6.2,*HR=*,F6.2,*HP=*,F4.1)
                8436  CONTINUE
                      STOP
  120                 END

      SUBROUTINE F        74/74   OPT=0   TRACE OEBUG              FTN 4.2+P380       05/20/75  10.31.49.       PAGE     1

                      SUBROUTINE F(THETA,TS,P)
                      DIMENSION TS(1),P(1)
                      COMMON AA,BB,CC
                      P(1)=AA-BB*TS(1)-CC*TS(1)**4
        5             RETURN
                      END
```

APPENDIX II
COMPUTER PROGRAM DAN

This appendix lists the computer program utilized to convert raw digital data tapes directly into time-temperature profile curves.

```
      PROGRAM DAN(INPUT,OUTPUT,TAPE1,TAPE7,TAPE6=OUTPUT,PLOT)
      DIMENSION IA(1500),IB(2000)
     1,IM(5)
      DIMENSION HOR(7),          ISF(9),MAS(9)
      DIMENSION IS (9),SEN(2000),RT1(14),RT2(14),
     1MILSEC(10),SEC(10),DAY(10),HRS(10),MIN(10)
     2,ISN(2000)
     3, T1(15), T2(15)
      DIMENSION S701(10),S702(10),S703(10),S704(10),S705(10),S706(10)
     1,S707(10),S121(10),S122(10),S123(10),S124(10),S125(10),S126(10)
     2,S127(10),S54(10)
     3,XR(400,16),DATA(1024)
     4,X1(400),Y1(400)
      INTEGER SEC,DAY,HRS
      DATA (RT1(I),I=1,14)/455.5,457.04,455.5,457.15,458.66,457.22,
     1457.09,457.32,457.35,457.20,456.94,457.08,459.30,456.30/
      DATA (RT2(I),I=1,14)/632.48,634.67,634.41,635.03,636.47,634.79,
     1634.59,634.85,634.44,634.65,634.20,634.25,637.26,634.01/
      DATA (MAS(I),I=1,7 )/00000000000000003779,
     100000000000000077779,00000000000000000378,
     200000000000000001778,00000000000000007779,
     300000000000000000778,00000000000000001779/
      DATA (IS (I),I=1,5 )/-16,-8,-11,-13,-7/
      DATA (ISF(I),I=1,9) /6,12,18,24,30,36,42,48,54/
      DELTA=1.493
      BETA =.111
      IO=0
      CALL PLOT(0.0,0.0,-3)
      X=900./255.
      Y= 9./5.
      LC=0
      LCT=0
      IREC=0
      ICT =0
      IC=0
      IR=0
      IFIL=0
       READ 40, ( T1(I),I=1,15)
   40 FORMAT(15F2.0)
       READ 41, ( T2(I),I=1,15)
   41 FORMAT(15F1.0)
      DO 36J=1,9
   36 ISF(J)=ISF(J)*(-1)
C ZERO THE IB ARRAY
  299 DO 300I=1,2000
  300 IB(I)=0
      ICNT=0
      J=1
      M=3
   25 BUFFER IN(1,1) (IA(1),IA(1500))
      IF(UNIT(1)) 301,302,303
  303 ICT = ICT + 1
      IREC=IREC+1
      PRINT 414 ,IREC
  414 FORMAT(31H PARITY ERROR IN RECORD NUMBER I5)
```

```
      GO TO 25
  301 INCT=INCT+1
      L=LENGTH(1)
      IF(LENGTH(1).GT.1499) GO TO 50
   60 IF(L.EQ.5) GO TO 51
      IREC=IREC+1
      DO 305K=1,L,4
      CALL MOVEF(8,IA,J,IB,M)
      J=J+8
   65 M=M+10
      CALL MOVEF(8,IA,J,IB,M)
      J=J+8
      M=M+10
      CALL MOVEF(8,IA,J,IB,M)
   70 J=J+8
      M=M+10
      CALL MOVEF(8,IA,J,IB,M)
      J=J+8
      M=M+10
   75 CALL MOVEF(8,IA,J,IB,M)
      J=J+8
      M=M+10
  305 CONTINUE
      IF(L.NE.1168) GO TO 310
   80 ICNT=(L*5)/4
      NN=ICNT
      KK=0
      KK=KK+1
      DO 306I=1,1440,12
   85 ISN(KK)   =AND(IB(I),MAS(1))
      ISN(KK+1)=AND(SHIFT(IB(I+11),IS (1)),MAS(1))
      ISN(KK+2)=AND(SHIFT(IB(I+11),IS (2)),MAS(1))
      ISN(KK+3)=AND(IB(I+11),MAS(1))
      KK=KK+4
   90 306 CONTINUE
      JJ=0
      DO 307M=1441,1460,2
      JJ=JJ+1
      SEC(JJ)   =AND(SHIFT(IB(M),IS (3)),MAS(6))
   95 MILSEC(JJ) =AND(IB(M),MAS(4))
      DAY(JJ)   =AND(SHIFT(IB(M+1),IS (4)),MAS(5))
      HRS(JJ)   =AND(SHIFT(IB(M+1),IS (5)),MAS(3))
      MIN(JJ)   =AND(IB(M+1),MAS(6))
  307 CONTINUE
  100 J=0
      DO 200I=1,480,48
      J=J+1
      RT=X*FLOAT(ISN(I+3))
      K=1
  105 RTT1=RT1(K)
      RTT2=RT2(K)
      CALL JOHN(RT,RTT1,RTT2,T)
      S701(J)=T*Y+492.
      RT=X*FLOAT(ISN(I+7))
  110 K=K+1
```

```
                RTT1=RT1(K)
                RTT2=RT2(K)
                CALL JOHN(RT,RTT1,RTT2,T)
                S702(J)=T*Y+492.
115             RT=X*FLOAT(ISN(I+11))
                K=K+1
                RTT1=RT1(K)
                RTT2=RT2(K)
                CALL JOHN(RT,RTT1,RTT2,Y)
120             S703(J)=T*Y+492.
                RT=X*FLOAT(ISN(I+15))
                K=K+1
                RTT1=RT1(K)
                RTT2=RT2(K)
125             CALL JOHN(RT,RTT1,RTT2,T)
                S704(J)=T*Y+492.
                RT=X*FLOAT(ISN(I+19))
                K=K+1
                RTT1=RT1(K)
130             RTT2=RT2(K)
                CALL JOHN(RT,RTT1,RTT2,T)
                S705(J)=T*Y+492.
                RT=X*FLOAT(ISN(I+23))
                K=K+1
135             RTT1=RT1(K)
                RTT2=RT2(K)
                CALL JOHN(RT,RTT1,RTT2,T)
                S706(J)=T*Y+492.
                K=K+1
140             RT=X*FLOAT(ISN(I+1))
                RTT1=RT1(K)
                RTT2=RT2(K)
                CALL JOHN(RT,RTT1,RTT2,T)
C  S7-7 REPRESENT 38-0
145             S707(J)=T*Y+492.
                K=K+1
                RT=X*FLOAT(ISN(I+27))
                RTT1=RT1(K)
                RTT2=RT2(K)
150             CALL JOHN(RT,RTT1,RTT2,T)
                S121(J)=T*Y+492.
                K=K+1
                RT=X*FLOAT(ISN(I+31))
                RTT1=RT1(K)
155             RTT2=RT2(K)
                CALL JOHN(RT,RTT1,RTT2,T)
                S122(J)=T*Y+492.
                K=K+1
                RT=X*FLOAT(ISN(I+35))
160             RTT1=RT1(K)
                RTT2=RT2(K)
                CALL JOHN(RT,RTT1,RTT2,T)
                S123(J)= T * Y +492.
                K=K+1
165             RT=X*FLOAT(ISN(I+39))
```

```
                RTT1=RT1(K)
                RTT2=RT2(K)
                CALL JOHN(RT,RTT1,RTT2,T)
                S124(J)= T * Y + 492.
170             K=K+1
                RT= X*FLOAT(ISN(I+43))
                RTT1=RT1(K)
                RTT2=RT2(K)
                CALL JOHN(RT,RTT1,RTT2,T)
175             S125(J)=T*Y+492.
                K=K+1
                RT= X*FLOAT(ISN(I+47))
                RTT1=RT1(K)
                RTT2=RT2(K)
180             CALL JOHN(RT,RTT1,RTT2,T)
                S126(J)=T*Y+492.
                K=K+1
                RT=X*FLOAT(ISN(I+5))
                RTT1=RT1(K)
185             RTT2=RT2(K)
                CALL JOHN(RT,RTT1,RTT2,T)
              C  S127 REPRESENT 38-1
                S127(J)=T*Y+492.
                S54(J)=X*FLOAT(ISN(I+26))
190          200  CONTINUE
                IF(LCT.EQ.0) PRINT 210,(IH(I),I=1,5)
             210  FORMAT(1H137X5(3XA10))
                LCT=LCT+20
                A1 = 0.
195             A2 = 0.
                A3 = 0.
                A4 = 0.
                A5 = 0.
                A6 = 0.
200             A7 = 0.
                A11= 0.
                A12= 0.
                A13= 0.
                A14= 0.
205             A15= 0.
                A16= 0.
                A17= 0.
                A24 = 0.
                DO 500J=1,10
210             A1 = A1 +S701(J)
                A2 = A2 +S702(J)
                A3 = A3 +S703(J)
                A4 = A4 +S704(J)
                A5 = A5 +S705(J)
215             A6 = A6 +S706(J)
                A7 = A7 +S707(J)
                A11= A11+S121(J)
                A12= A12+S122(J)
                A13= A13+S123(J)
220             A14= A14+S124(J)
```

```
      A15= A15+S125(J)
      A16= A16+S126(J)
      A17= A17+S127(J)
  500 A54= A54+S54(J)
225   A1 = A1 /10.0
      A2 = A2 /10.0
      A3 = A3 /10.0
      A4 = A4 /10.0
      A5 = A5 /10.0
230   A6 = A6 /10.0
      A7 = A7 /10.0
      A11= A11/10.0
      A12= A12/10.0
      A13= A13/10.0
235   A14= A14/10.0
      A15= A15/10.0
      A16= A16/10.0
      A17= A17/10.0
      A54 =A54/10.
240   IF(LC.EQ.0) WRITE (7,210)
      IF(LC.EQ.0) WRITE (7,201)
  201 FORMAT(1H047H  7-1    12-1   7-2    12-2   7-3    12-3   7-7
     1,51H      7-4    12-4   7-5    12-5   7-6    12-6   12-7
     2,28H      54-6   DAY HR  M  S MS)
245   WRITE (7,202) A1,A2,A3,A4,A5,A6,A7,A11,A12,A13,A14,A15,A16,A17,
     1A54,DAY(5),HRS(5),MIN(5),SEC(5),MILSEC(5)
  202 FORMAT(1H0F6.1,6F7.1,F8.1,6F7.1,5XF5.1,3XI3,3I3,I4)
      LC=LC+2
      IF(LC.GE.50) LC=0
250   IFIL=IFIL+1
      IF(IQ.EQ.1) GO TO 299
      IF(IFIL.EQ.3) GO TO 600
      GO TO 299
  600 CONTINUE
255   IC=1
      IR=IR+1
      XR(IR,IC) = A1
      XR(IR,IC+ 1)= A2
      XR(IR,IC+ 2)= A3
260   XR(IR,IC+ 3)= A4
      XR(IR,IC+ 4)= A5
      XR(IR,IC+ 5)= A6
      XR(IR,IC+ 6)= A7
      XR(IR,IC+ 7)= A11
265   XR(IR,IC+ 8)= A12
      XR(IR,IC+ 9)= A13
      XR(IR,IC+10)= A14
      XR(IR,IC+11) =A15
      XR(IR,IC+12) =A16
270   XR(IR,IC+13) =A17
      XR(IR,IC+14)=A54
      ISEC=SEC(5)
      IHRS=HRS(5)
      IMIN=MIN(5)
275   NTIME=0
```

```
      XSEC=FLOAT(ISEC)
      XHRS=FLOAT(IHRS)
      XMIN=FLOAT(IMIN)
      TIME=XHRS+XMIN/60.+XSEC/3600.
280   XR(IR,IC+15)=TIME
      IF(IR.GE.398) GO TO 610
      IFIL=0
      GO TO 299
  610 PRINT 611
285   611 FORMAT(*1 MORE THAN 398 PTS ONLY 398 WILL BE PLOTTED.*)
      IQ=1
      GO TO 299
   50 WRITE (6,102)
  102 FORMAT(1H031HRECORD LENGTH GREATER THAN 1500)
290   STOP
  302 ENDFILE 6
      PRINT 104 , ICT
  104 FORMAT(29H THE NUMBER OF PARITY ERRORS ,I4)
      PRINT 103
295   103 FORMAT(24H END OF FILE ENCOUNTERED)
      GO TO 30
C GET HEADER RECORD
   51 PRINT 100,(IA(IJ),IJ=1,5)
  100 FORMAT(1H028X10HBCD RECORD/1H05(3XA10))
300   CALL MOVEF(50,IA,1,IH,1)
      GO TO 25
  310 PRINT 413 , IREC
  413 FORMAT(15H RECORD NUMBER I5,32H IS TOO SHORT ... RECORD SKIPPED)
      PRINT 110 ,(IA(I),I=1,L)
335   110 FORMAT(1H06(2X020))
      GO TO 299
   30 PRINT 107
  107 FORMAT(* RUN COMPLETE    *)
      N=IR
310   WRITE (6,700) ((XR(I,J),J=1,16),I=1,N)
  700 FORMAT(15(2XF5.1),2XF7.3)
      DO 601I=1,N
  601 X1(I)=XR(I,16)
      Y1(N+1)=380.
315   Y1(N+2)=20.
      IJK= IFIX(X1(1)*10.)
      X1(N+1)= FLOAT(IJK)/10.
      X1(N+2)=.1
      DO 603I=1,15
320   TN1=T1(I)
      TN2=T2(I)
      DO 602J=1,N
      Y1(J)=XR(J,I)
  602 CONTINUE
325   CALL AXIS(0.0,0.0,16HTIME HRS/MIN/SEC,-16,10.,0.,X1(N+1),X1(N+2))
      CALL AXIS(0.0,0.0,14HDEGREES RANKIN,14,9.,90.,Y1(N+1),Y1(N+2))
      CALL FLINE(X1,Y1,N,1,10,1)
      CALL NUMBER(2.0,9.0,.15,TN1,0.0,-1)
      CALL SYMBOL(999.,999.,.15,3H - ,0.0,3)
330   CALL NUMBER(999.,999.,.15,TN2,0.0,-1)
```

```
PROGRAM     DAN                                  CDC 6600 FTN V3.0-367A OPT=1  02/05/74  21.41.28.      PAGE      7

            CALL PLOT(22..0.0,-3)
          503  CONTINUE
            CALL PLOTE
            END


SUBROUTINE  JOHN                                 CDC 6600 FTN V3.0-367A OPT=1  02/05/74  21.41.28.      PAGE      1

            SUBROUTINE JOHN (RT,R0,R100,T)
            TRY=100.*((RT-R0)/(R100-R0))
          1 A=TRY/100.0
            T=100.0*((RT-R0)/(R100-R0))+1.493*(A-1.0)*A+0.111*(A-1.0)*(TRY**3/
 5         110.0**6 )
            TMT=T-TRY
            IF(ABS(TMT).LE..10) GO TO 2
            TRY=TRY+((T-TRY)/2.)
            GO TO 1
10        2 RETURN
            END
```

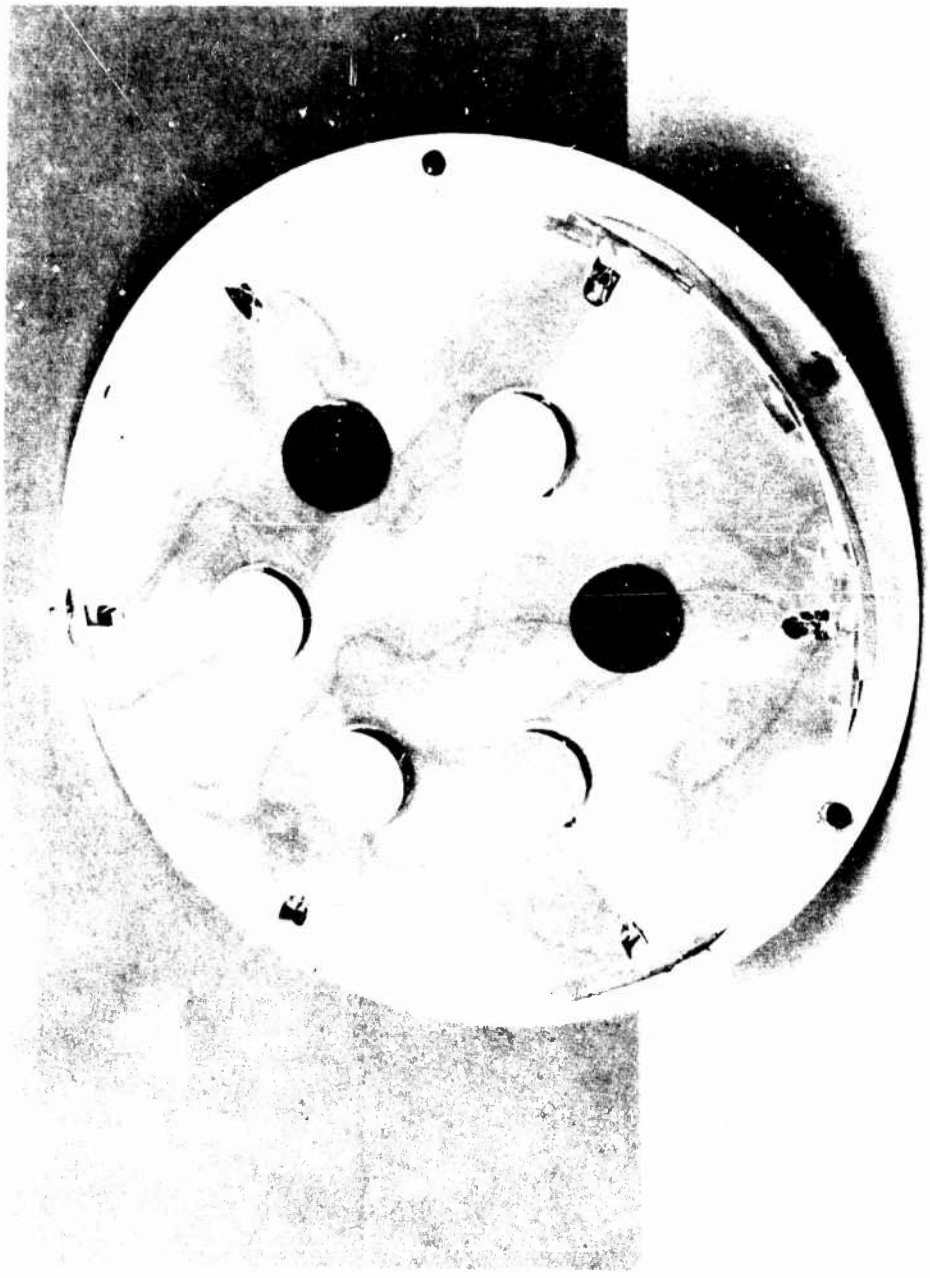

Figure 1. ML-101 Sample Holder

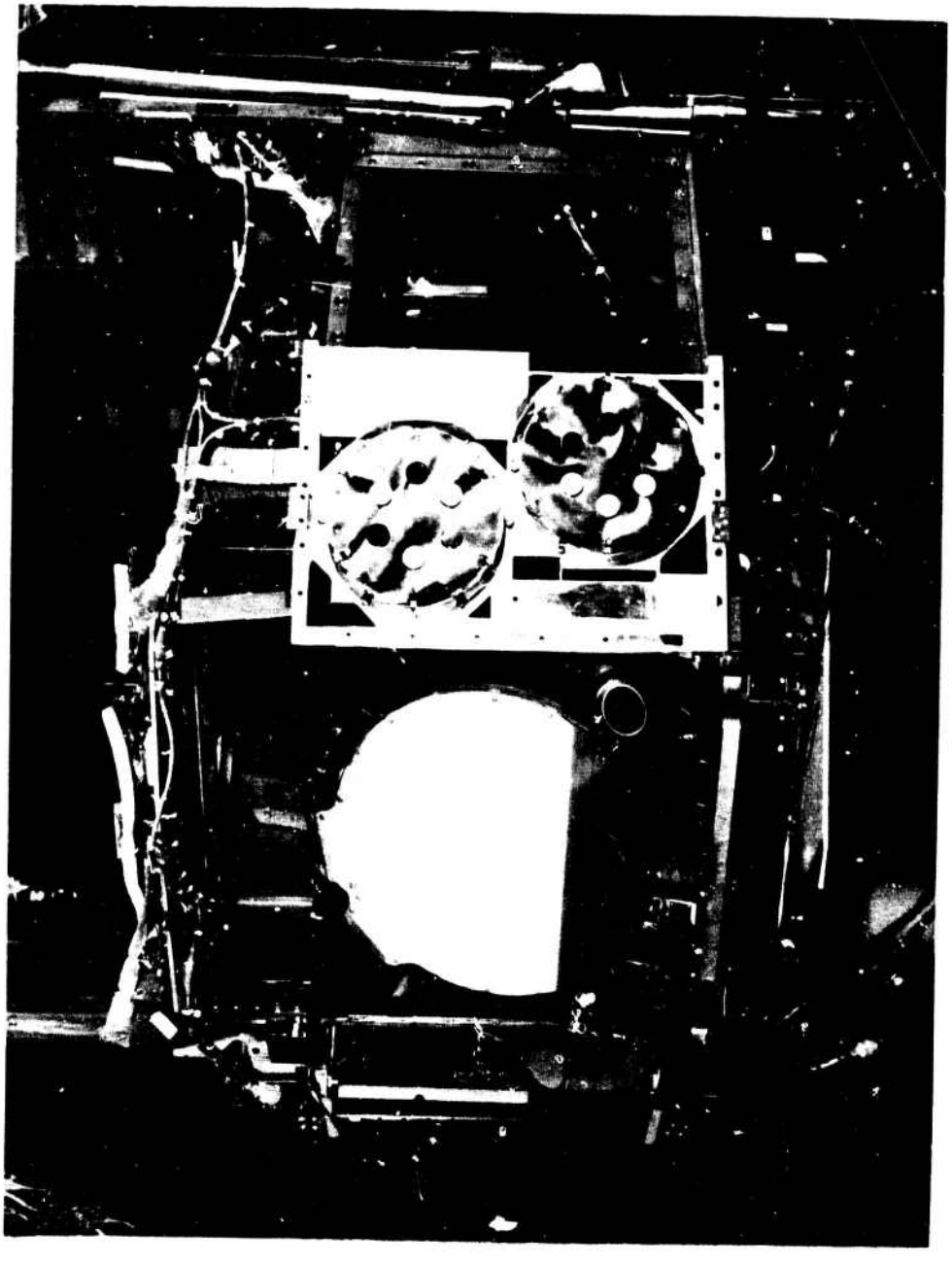

Figure 2. ML-101 Sample Holders Attached to 72-1 Satellite

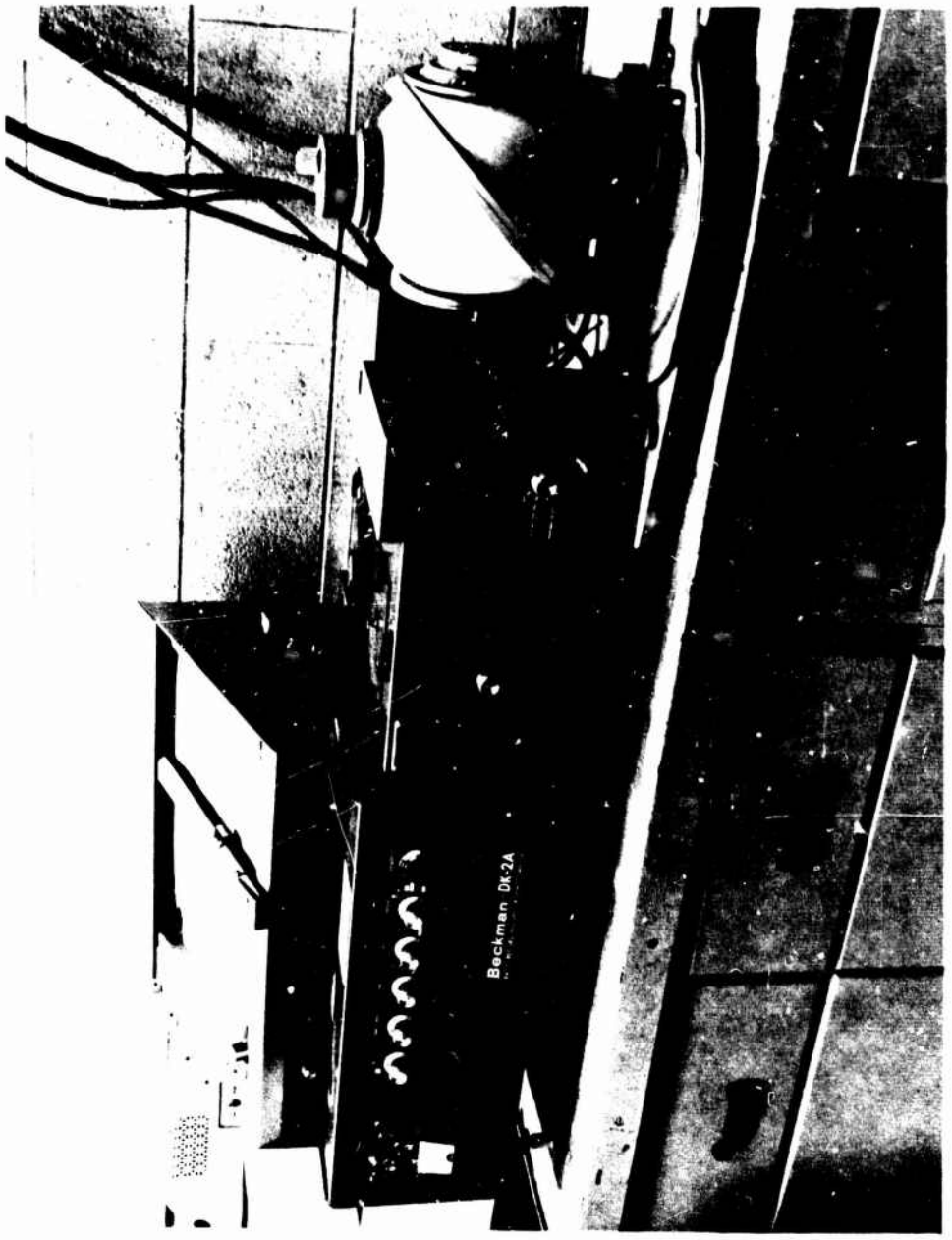

Figure 3. Beckman DK-2A Spectrophotometer with a Gier-Dunkle Absolute Integrating Sphere

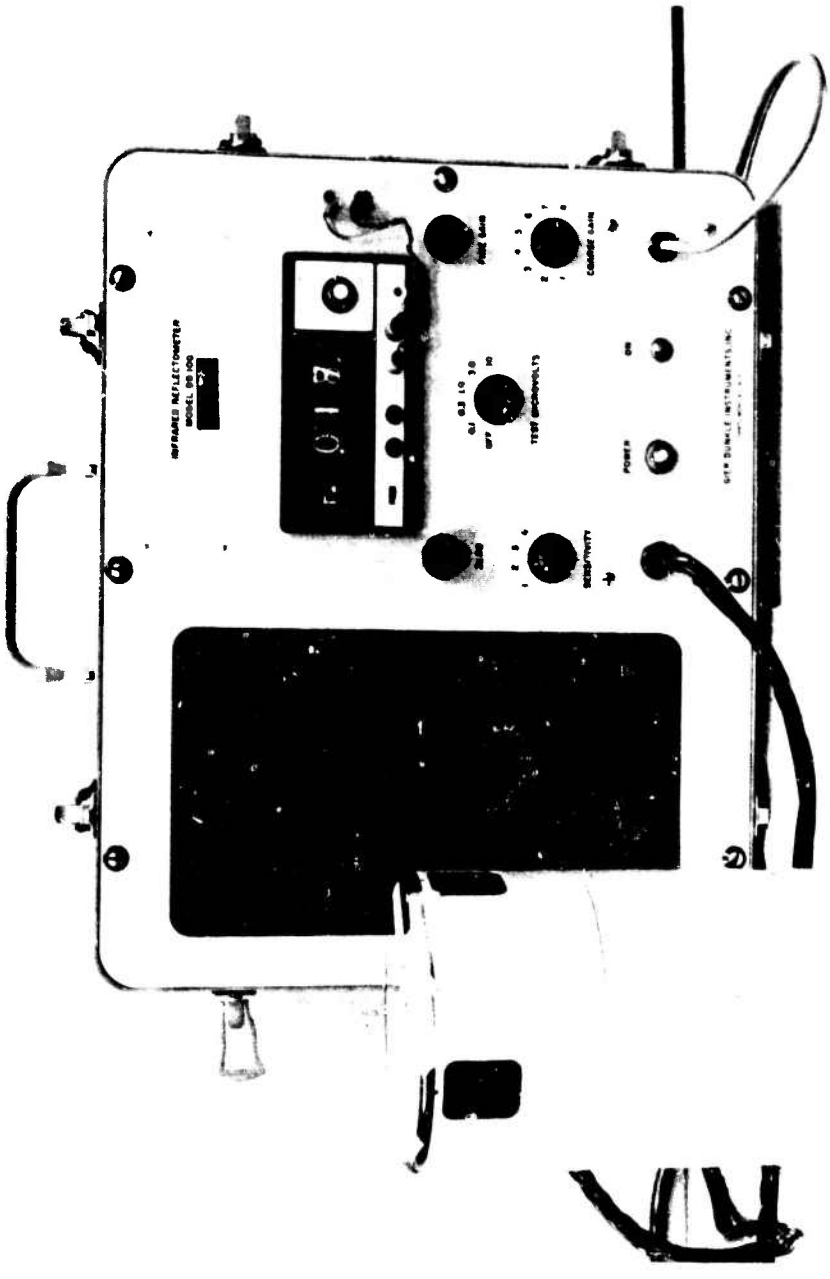

Figure 4. Gier-Dunkle Model DB100 Portable Infrared Reflectometer

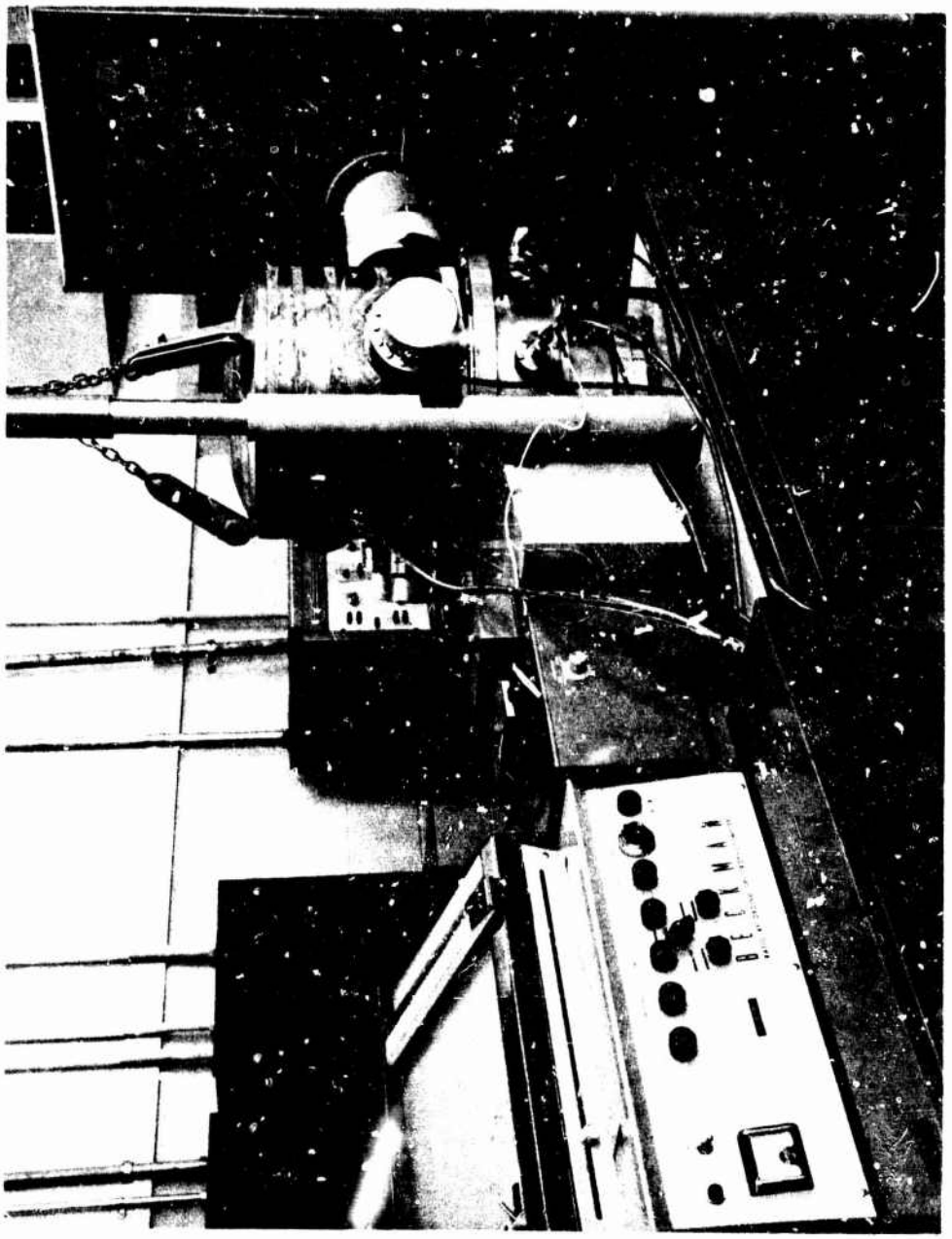

Figure 5. AFML In-Situ Exposure Device

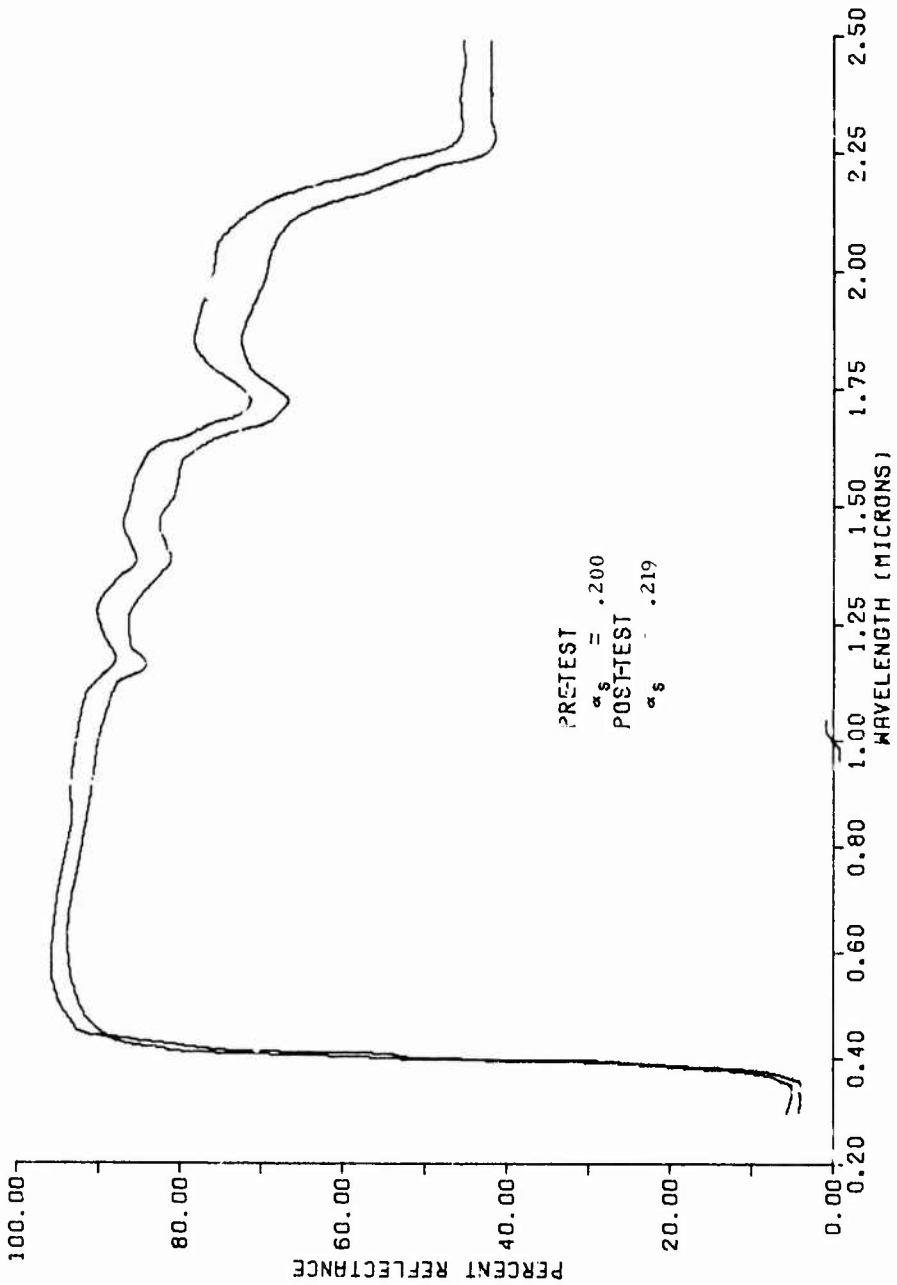

Figure 6. ML-101 Simulation Experiment S-15G (500 EUVSH)

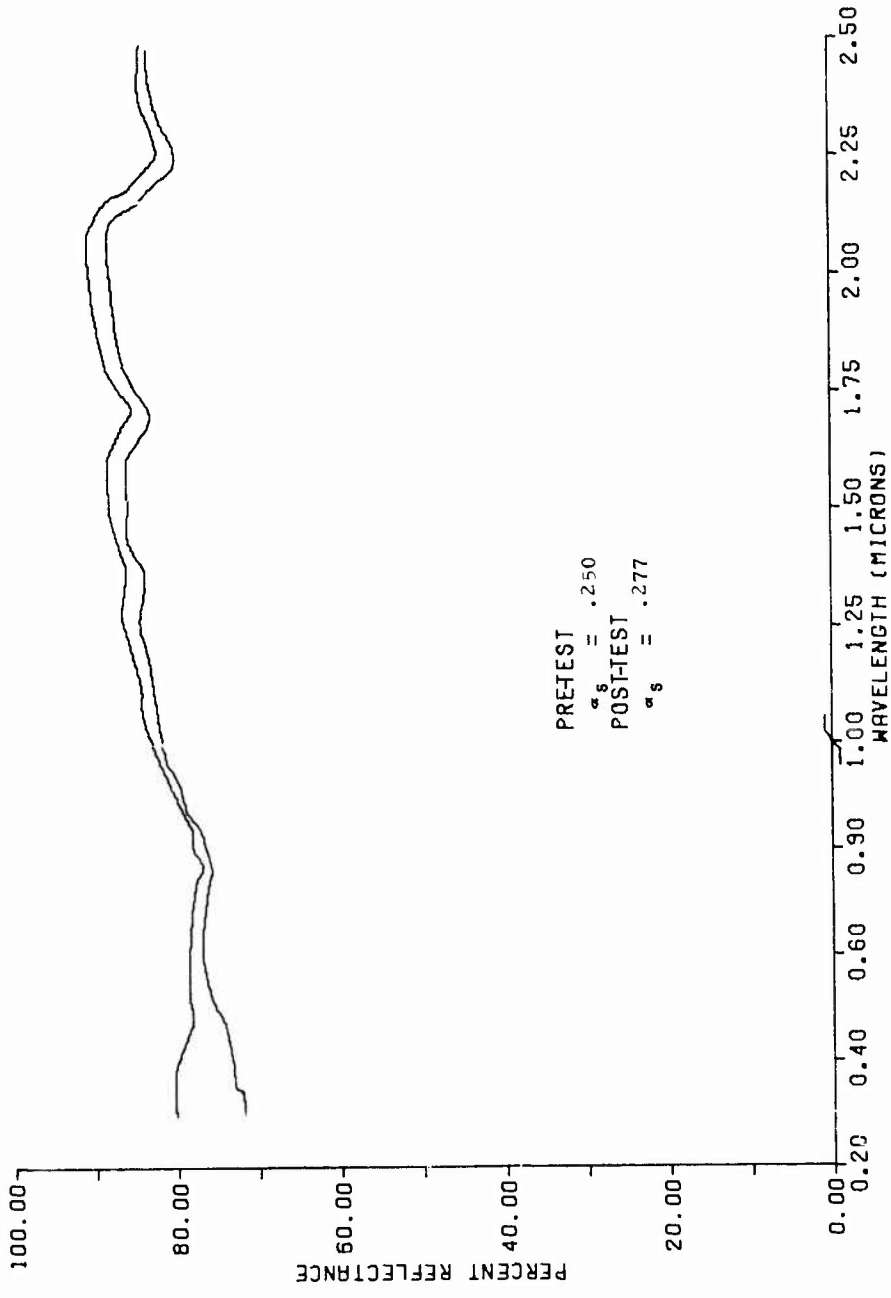

Figure 7. ML-101 Simulation Experiment SiO_2 Fabric (500 EUVSH)

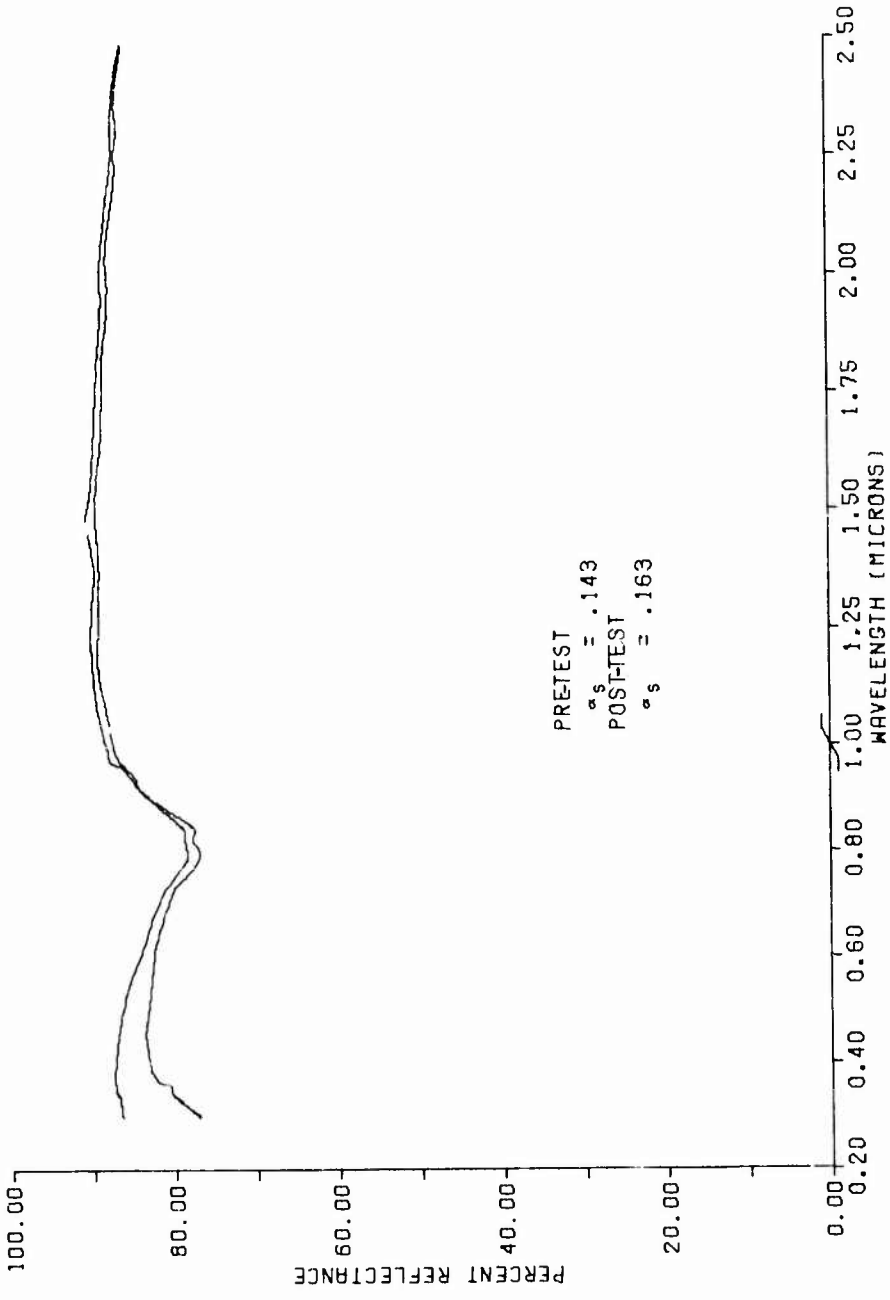

Figure 8. ML-101 Simulation Experiment FEP/Al (500 EUVSH)

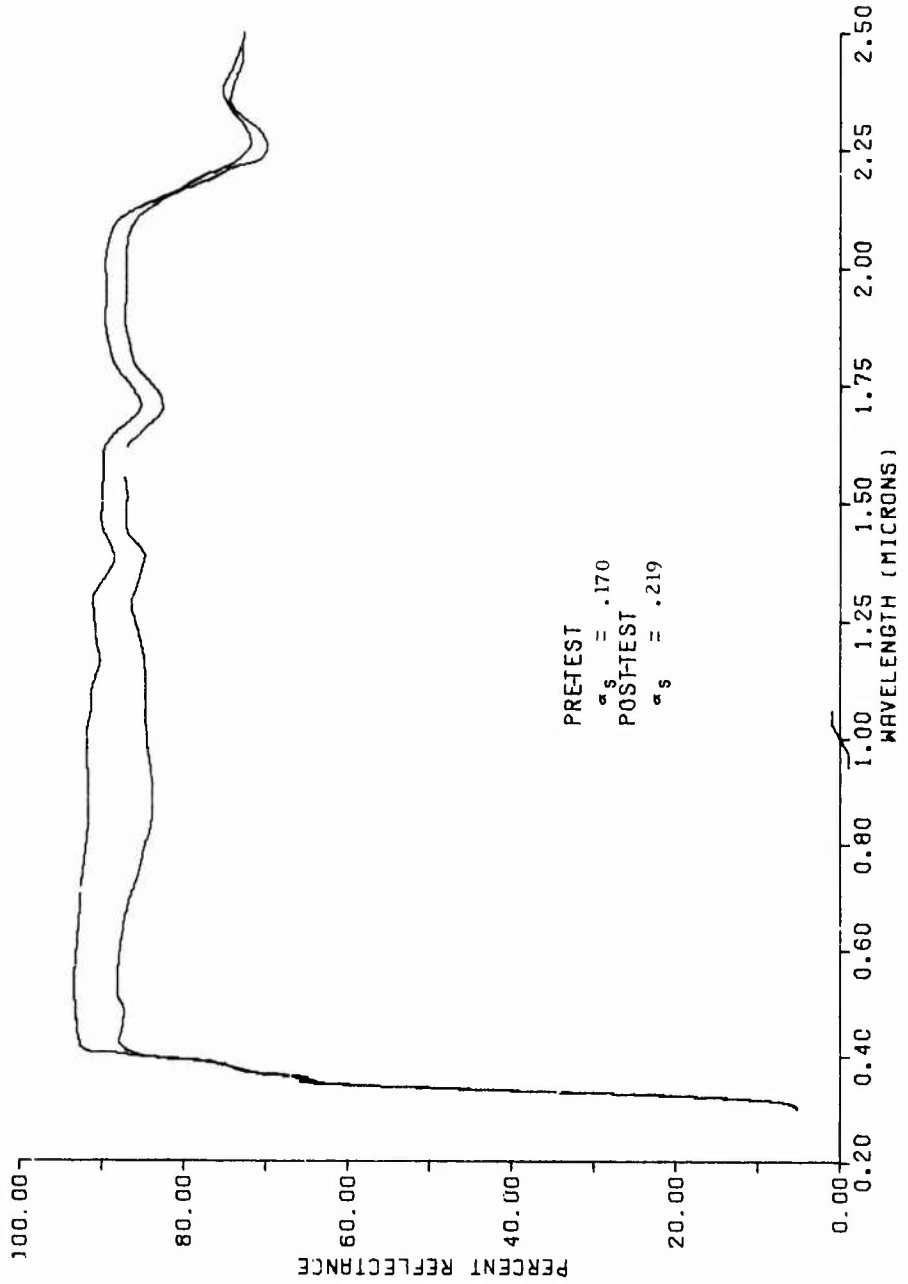

Figure 9. ML-101 Simulation Experiment Zr_2TiO_4/OI650 (500 EUVSH)

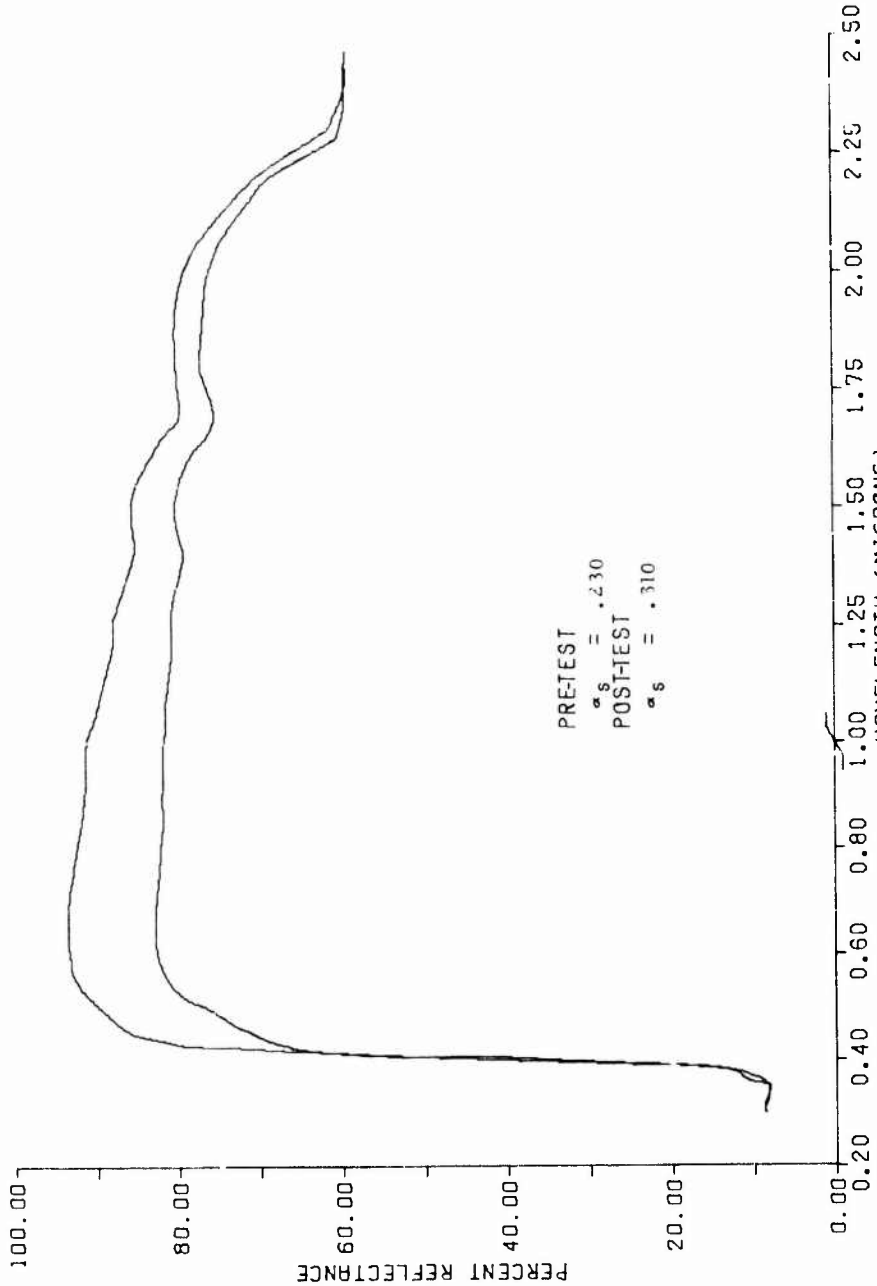

Figure 10. ML-101 Simulation Experiment PV-100 (500 EUVSH)

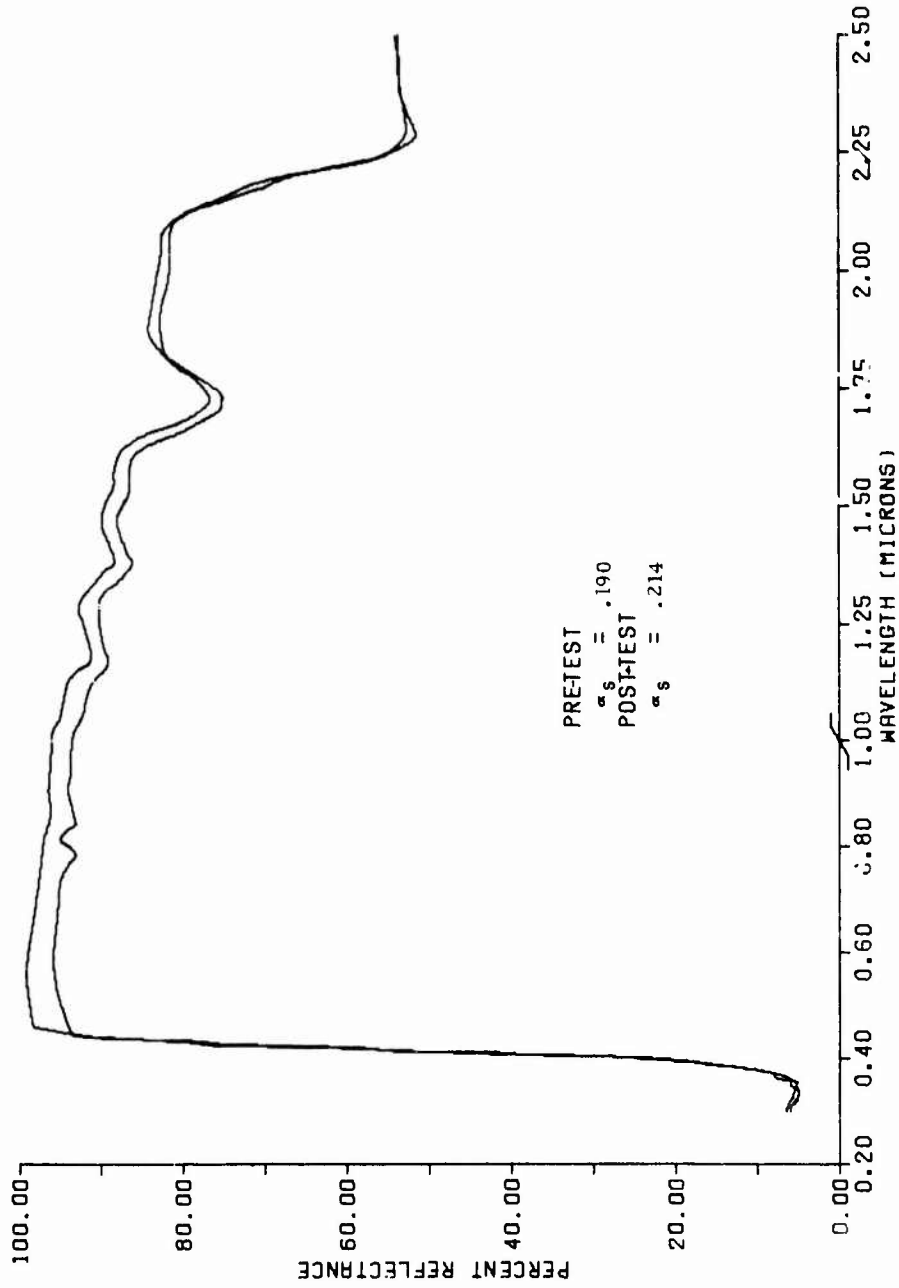

Figure 11. ML-101 Simulation Experiment TiO_2/RTV602 (500 EUVSH)

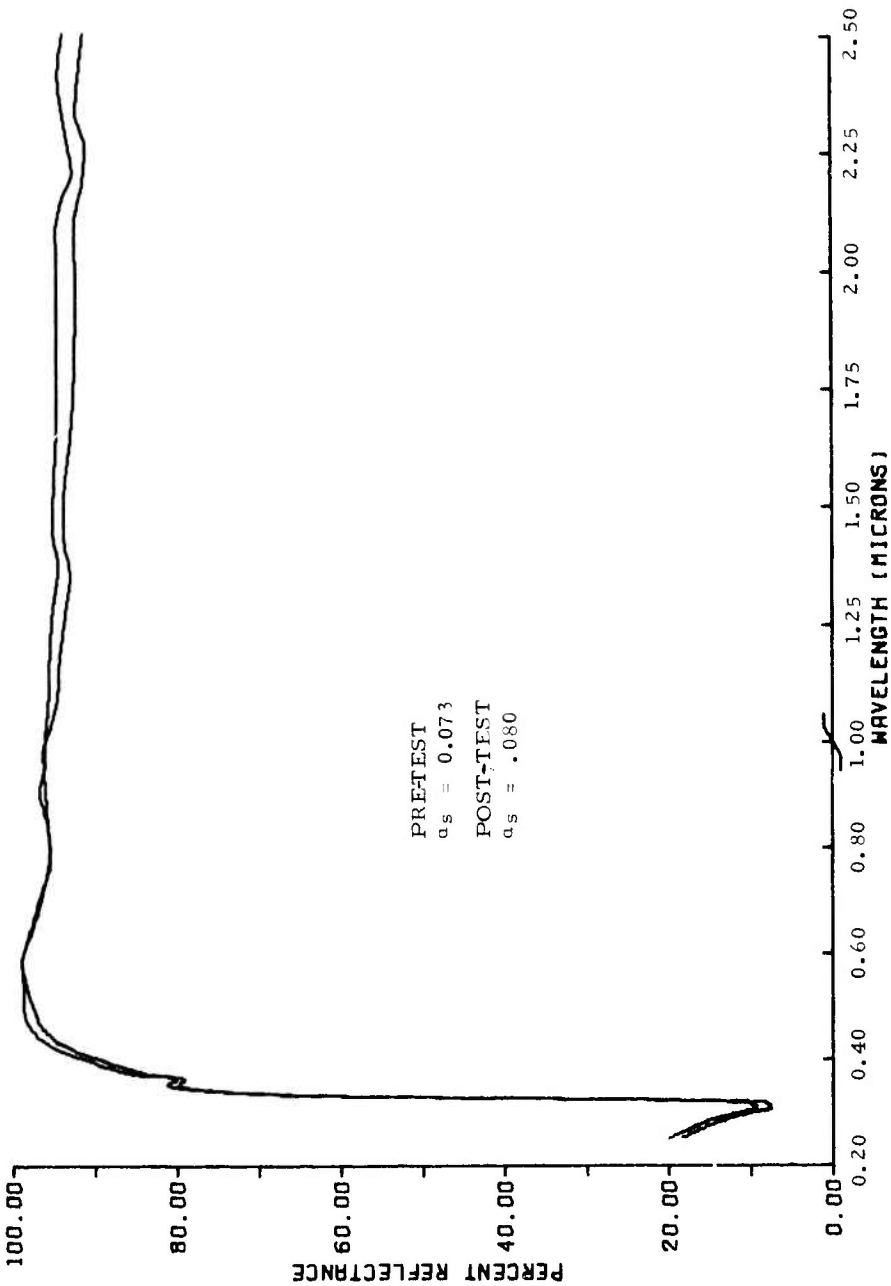

Figure 12. ML-101 Simulation Experiment .008" OSR (500 EUVSH)

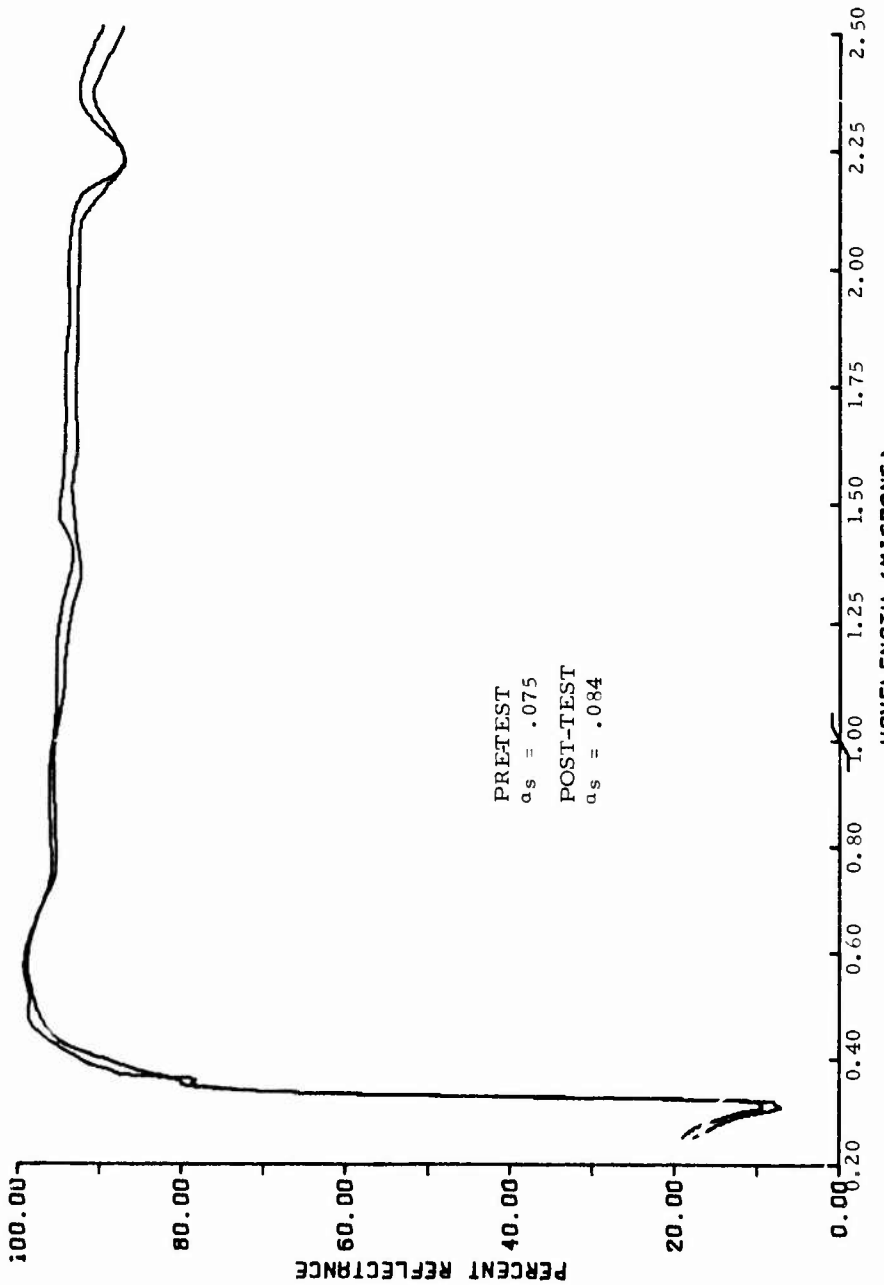

Figure 13. ML-101 Simulation Experiment .050" OSR (500 EUVSH)

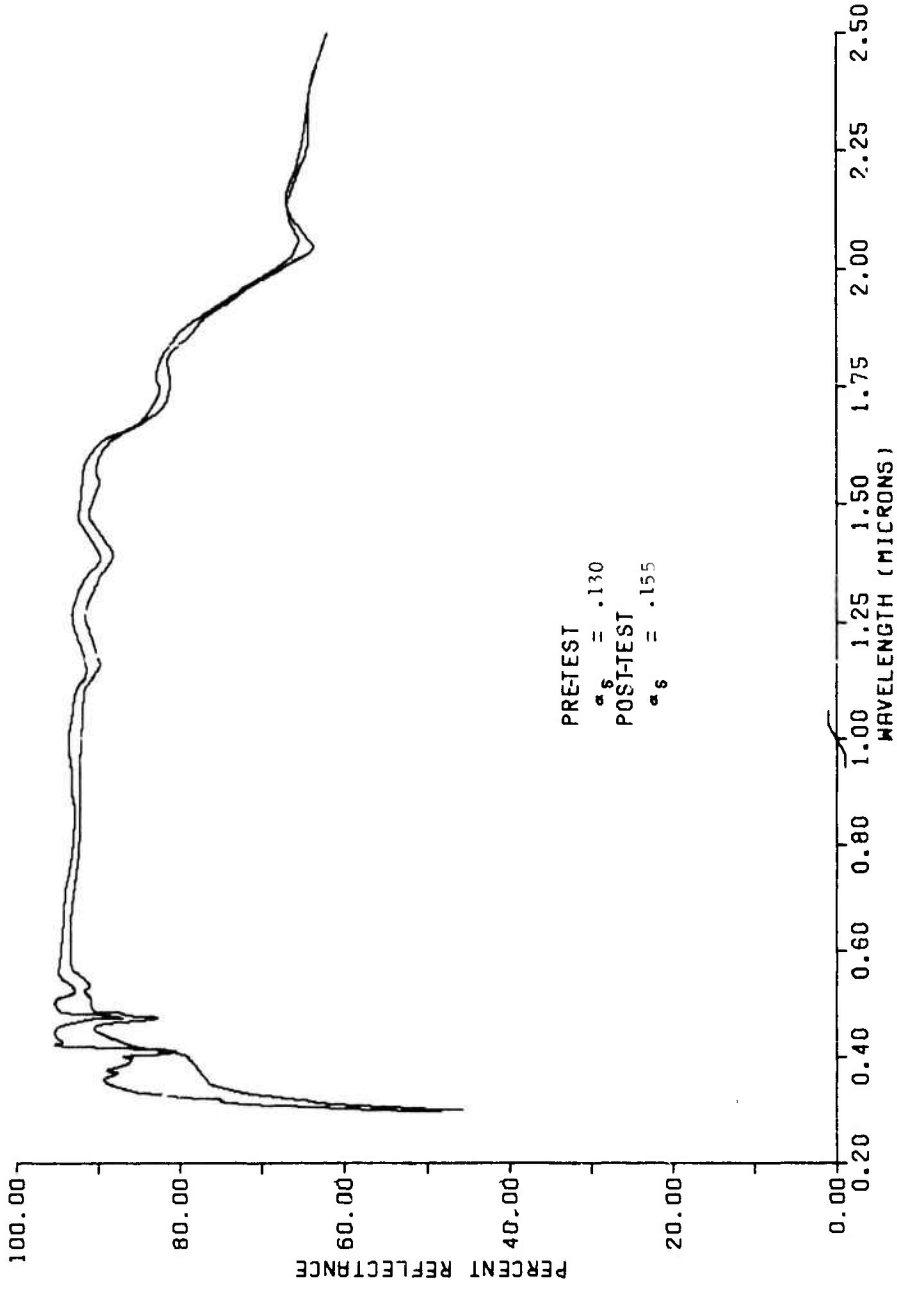

Figure 14. ML-101 Simulation Experiment Eu_2O_3/RTV602 (500 EUVSH)

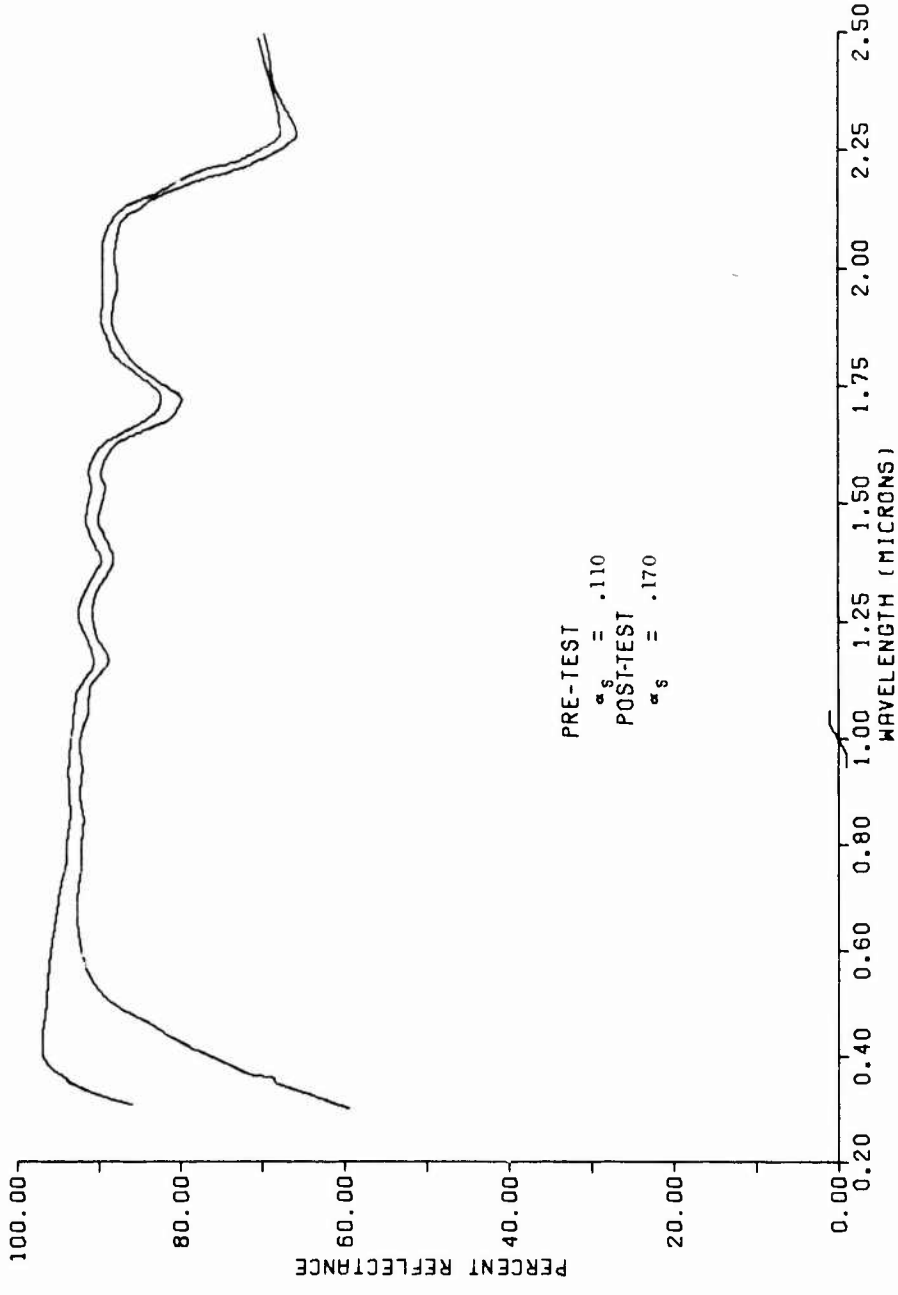

Figure 15. ML-101 Simulation Experiment Al_2O_3/RTV602 (500 EUVSH)

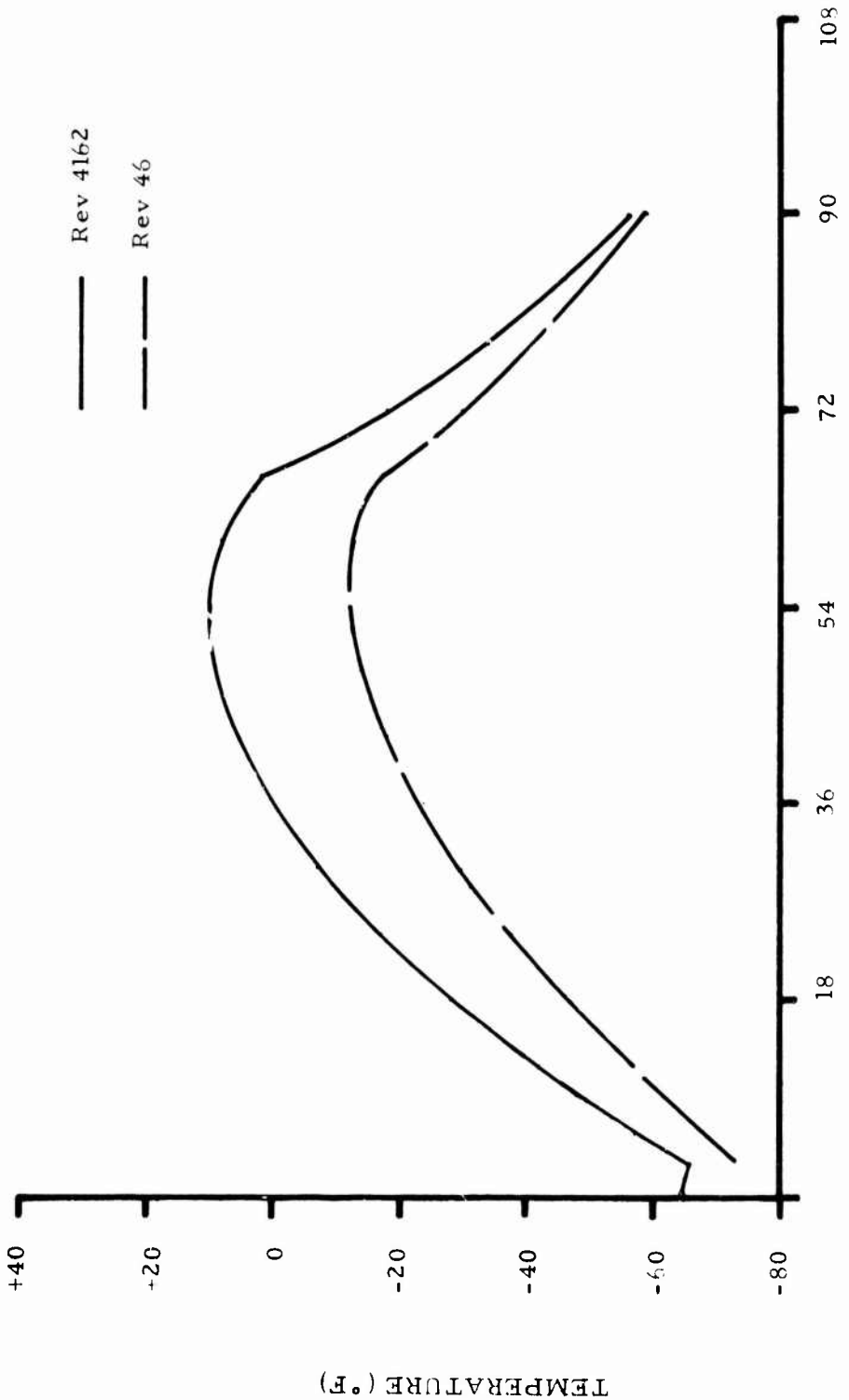

Figure 16. Sensor Temperature vs Time for S-13G During Revolutions 46 and 4162

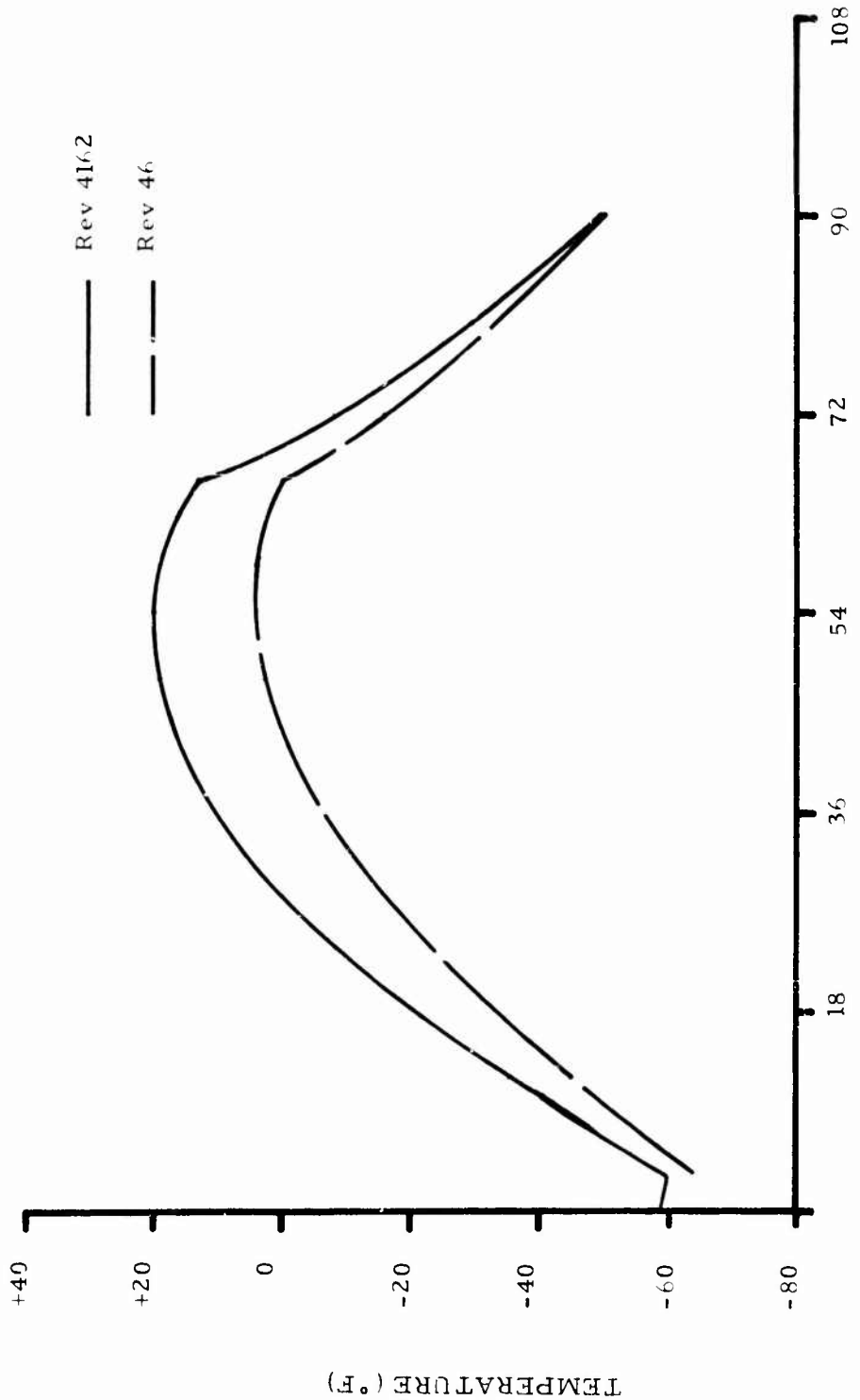

Figure 17. Sensor Temperature vs Time for SiO_2 Fabric During Revolutions 46 and 4162

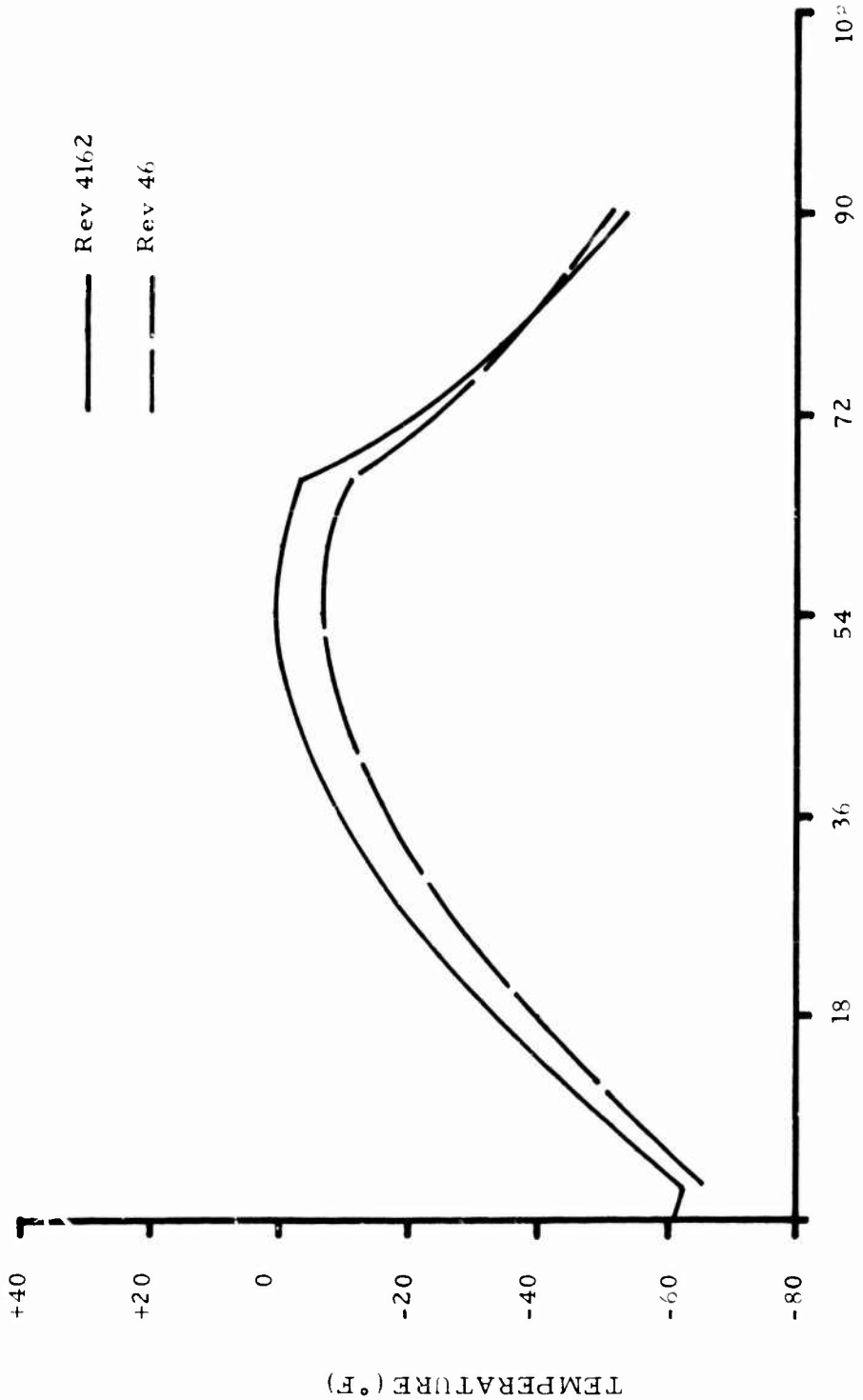

Figure 18. Sensor Temperature vs Time for FEP/Al During Revolutions 46 and 4162

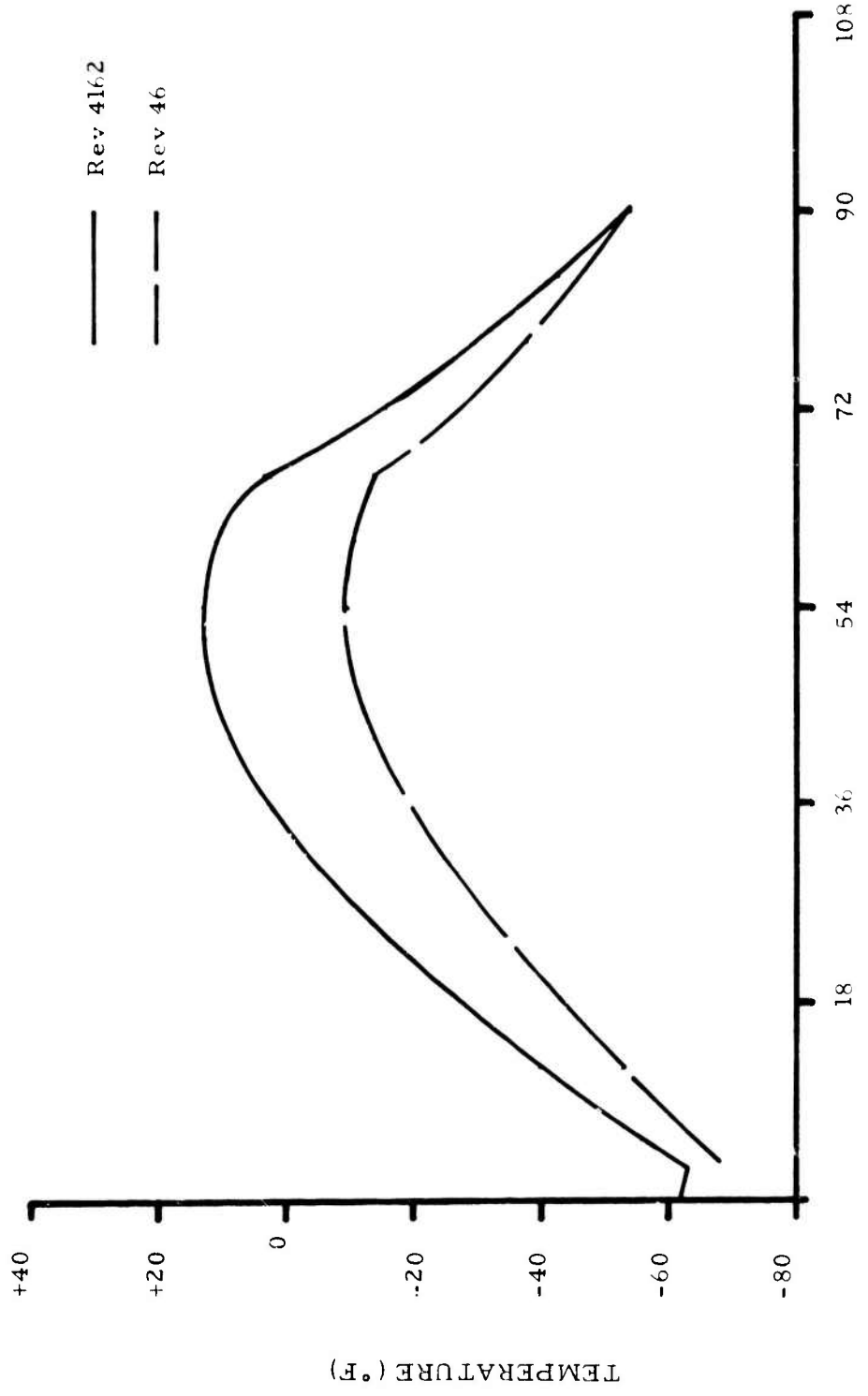

Figure 19. Sensor Temperature vs Time for Zn_2TiO_4/OI650 During Revolutions 46 and 4162

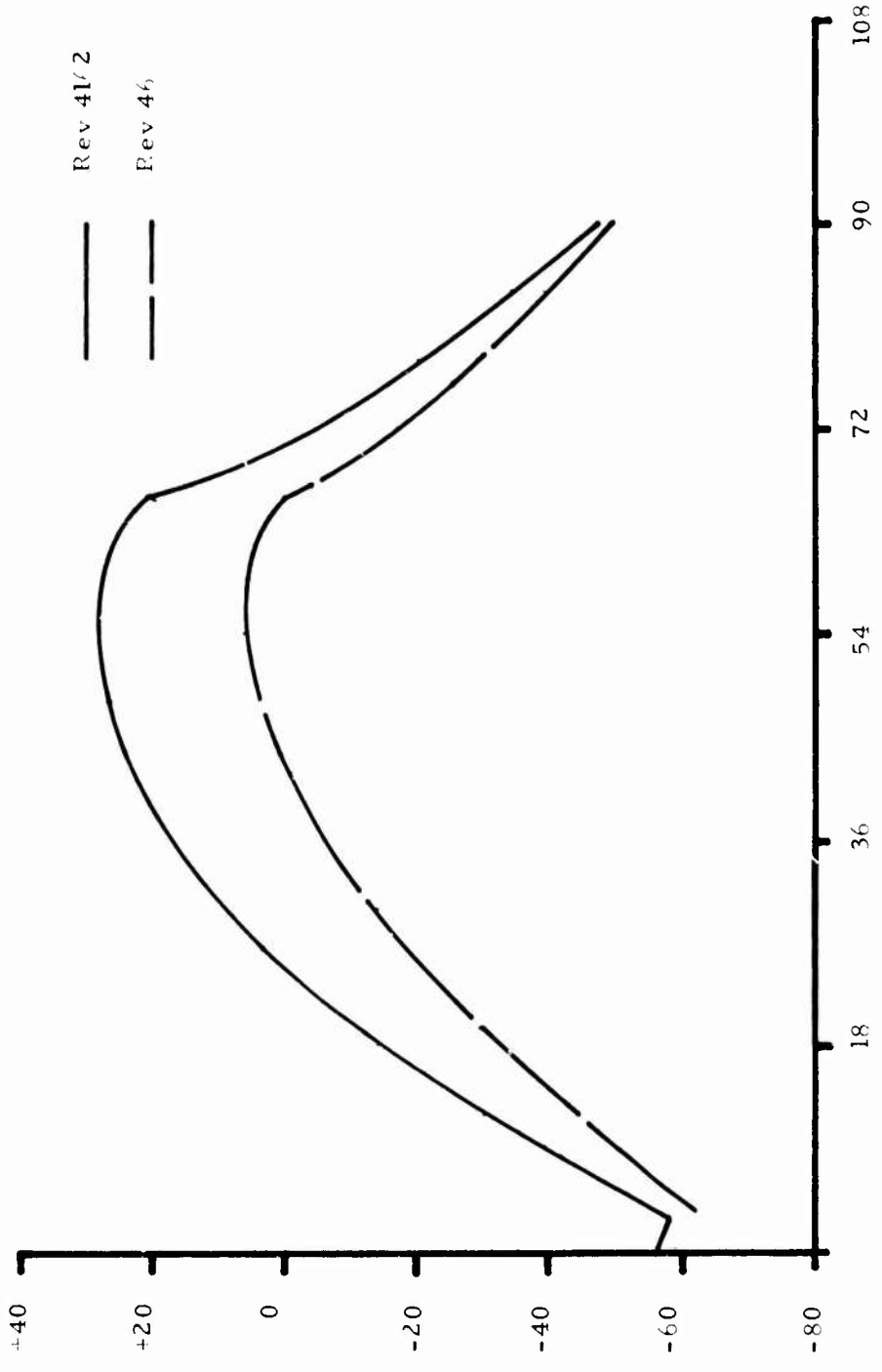

Figure 20. Sensor Temperature vs Time for PV-100 During Revolutions 46 and 4162

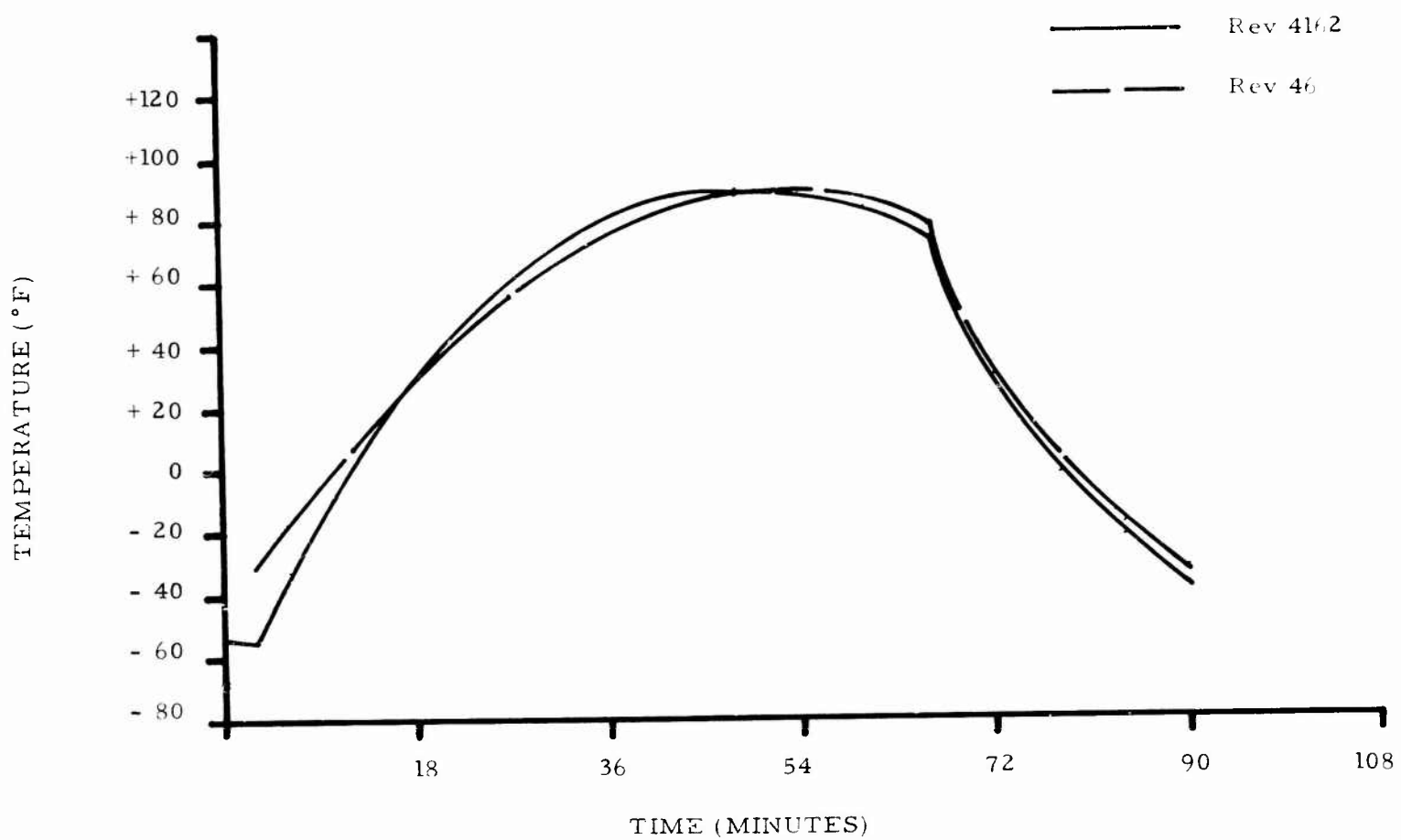

Figure 21. Sensor Temperature vs Time for 3M Black Velvet During Revolutions 46 and 4162

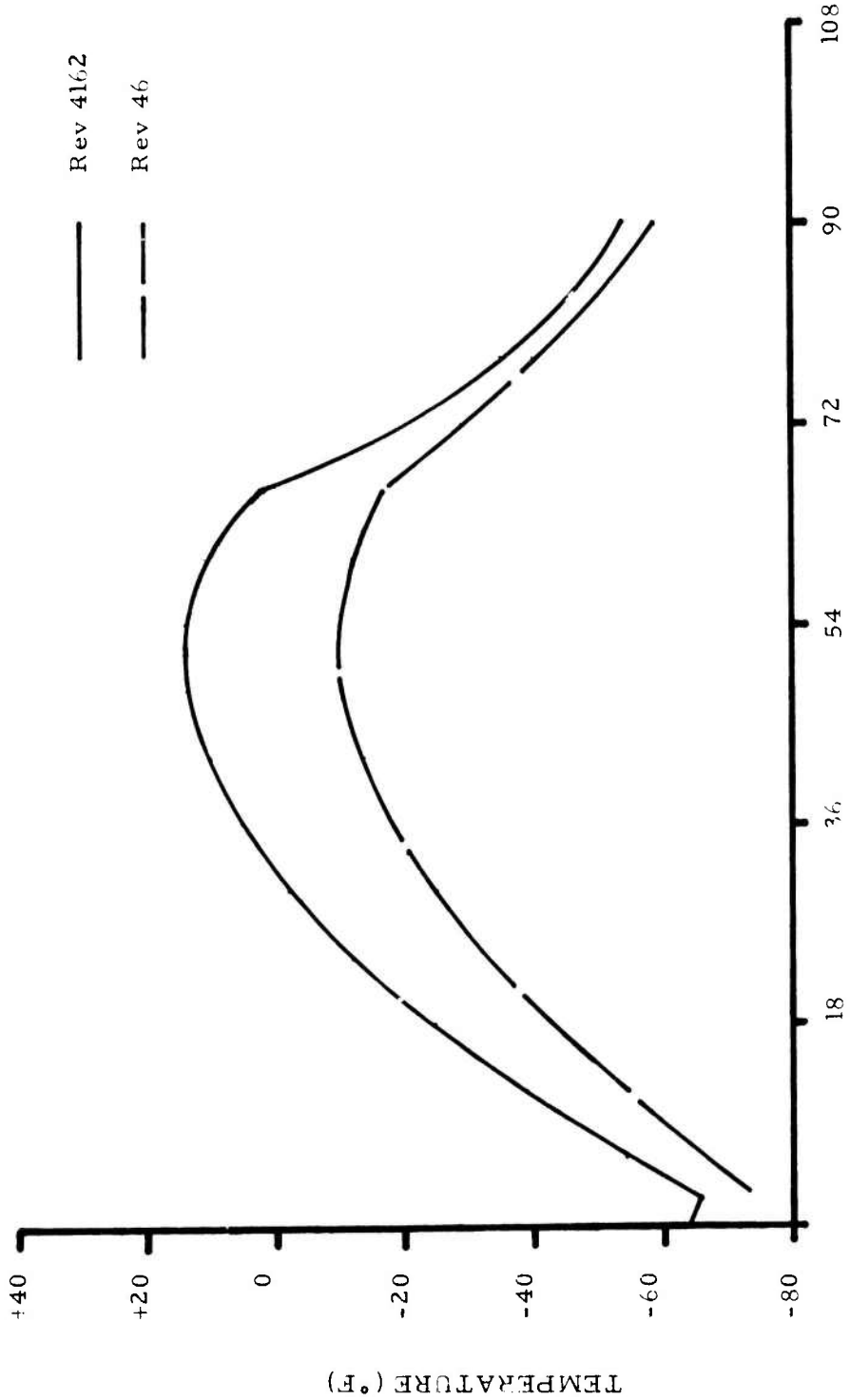

Figure 22. Sensor Temperature vs Time for TiO_2/Silicone During Revolutions 46 and 4162

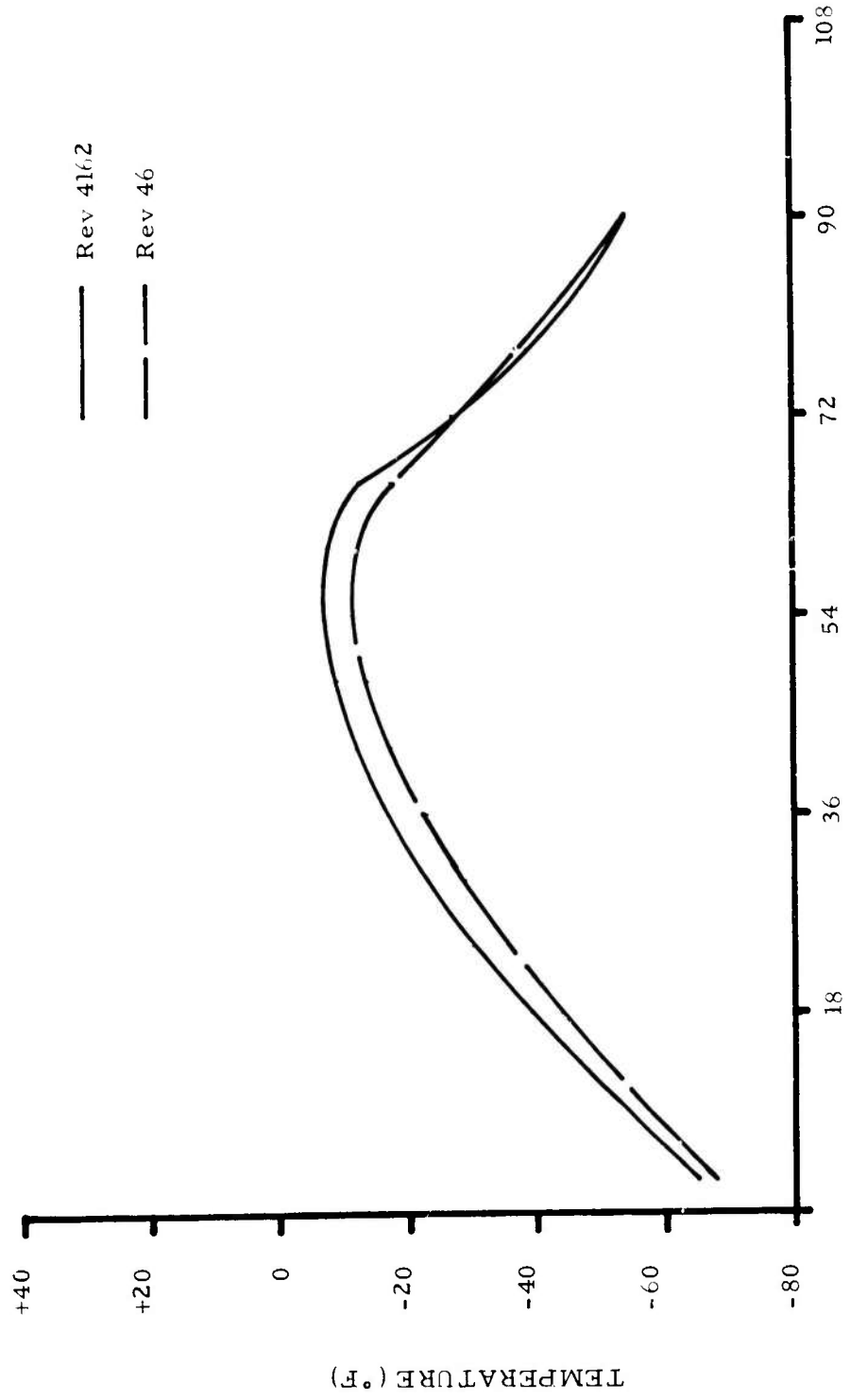

Figure 23. Sensor Temperature vs Time for OSR (0.008) During Revolutions 46 and 4162

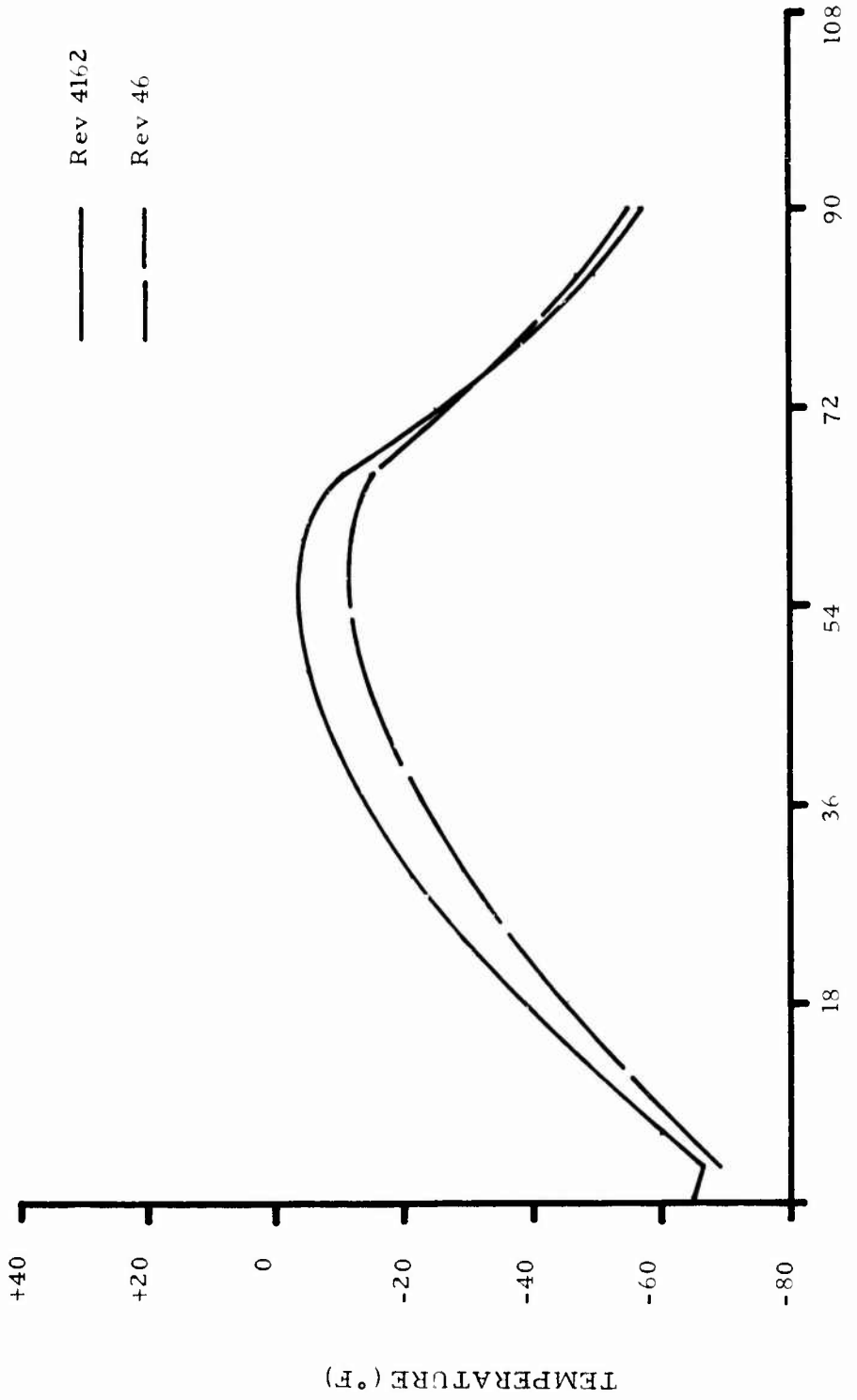

Figure 24. Sensor Temperature vs Time for OSR (0.050) During Revolutions 46 and 4162

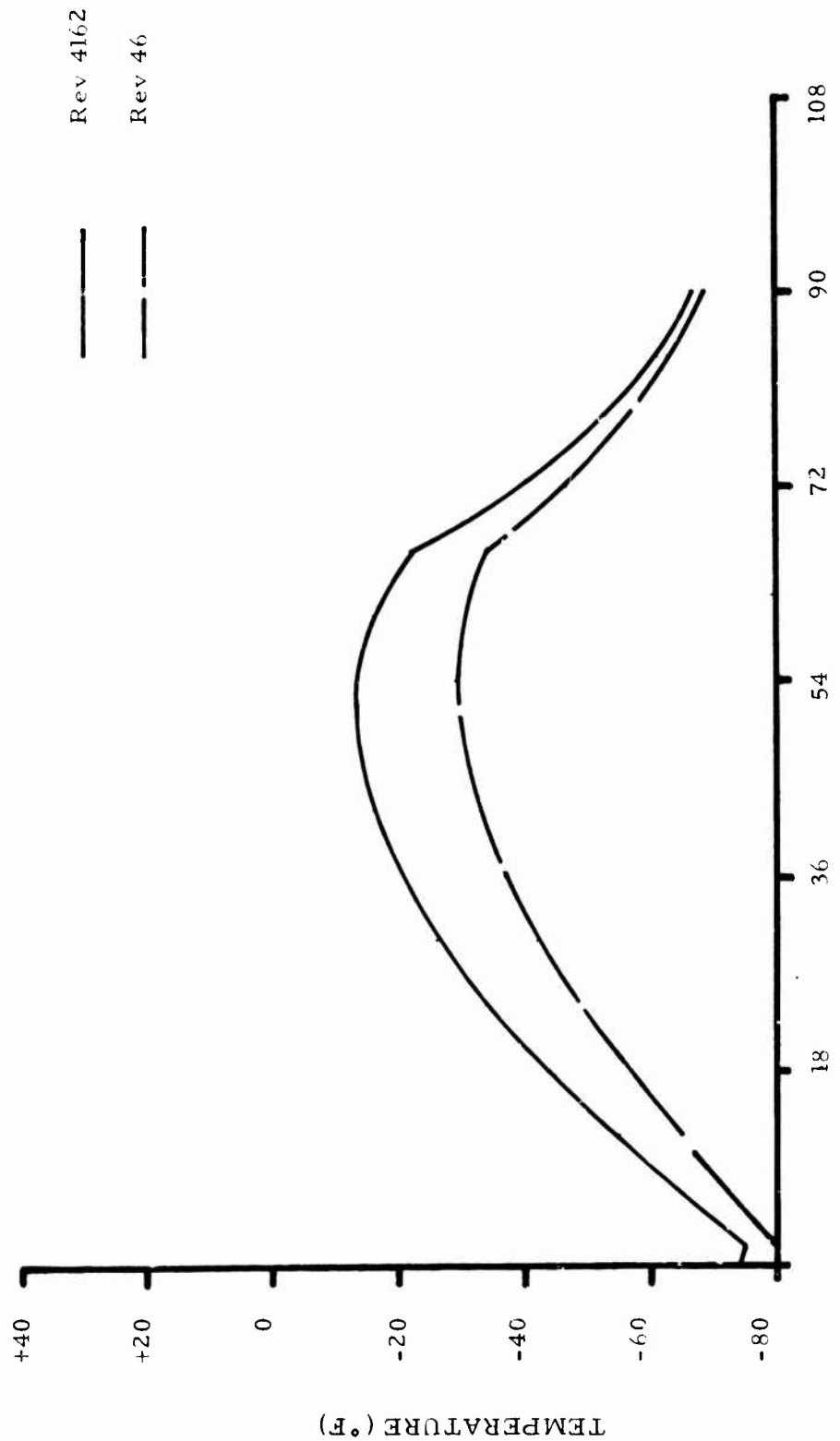

Figure 25. Sensor Temperature vs Time for Eu_2O_3/Silicone During Revolutions 46 and 4162

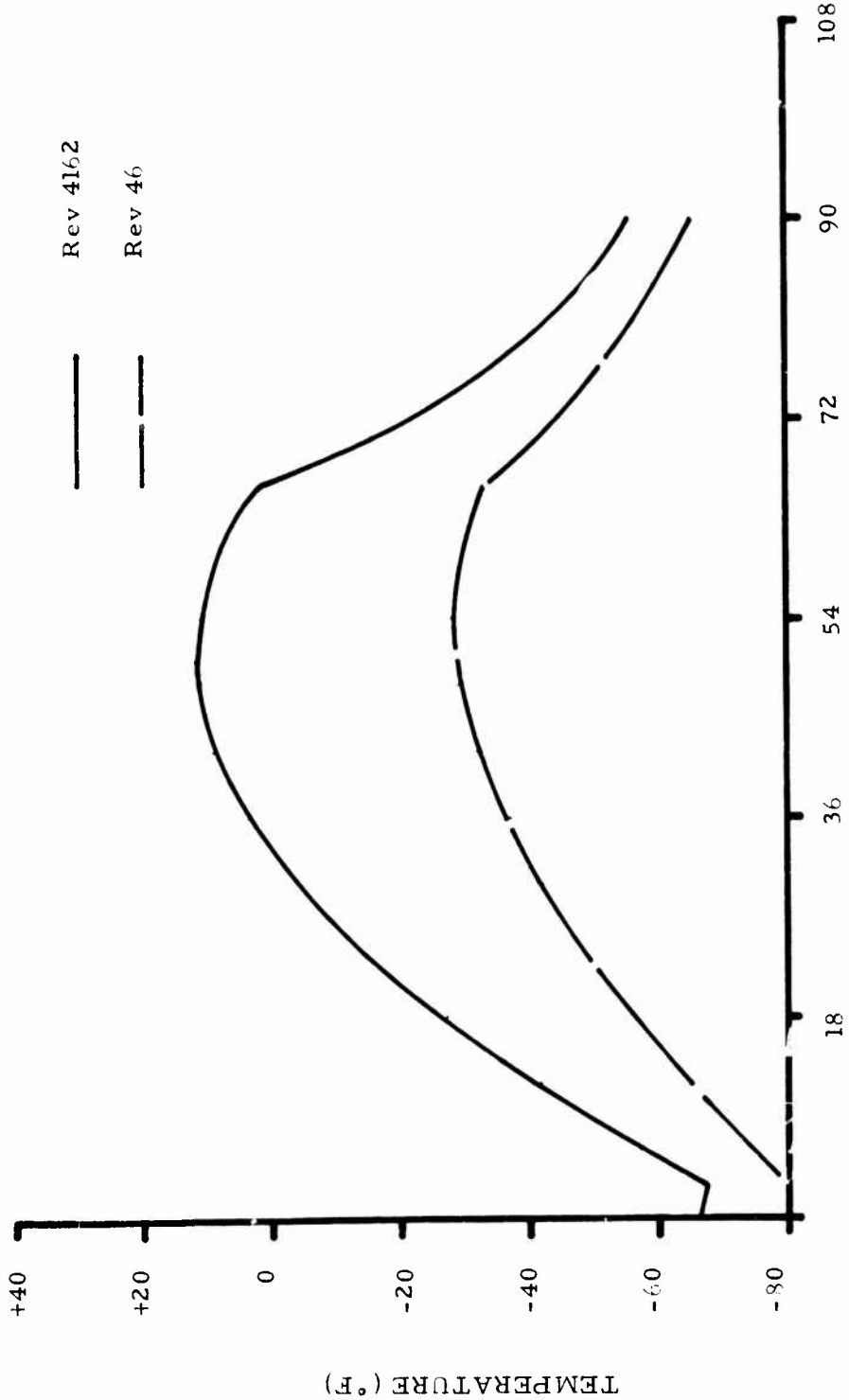

Figure 26. Sensor Temperature vs Time for α-Al_2O_3/Silicone During Revolutions 46 and 4162

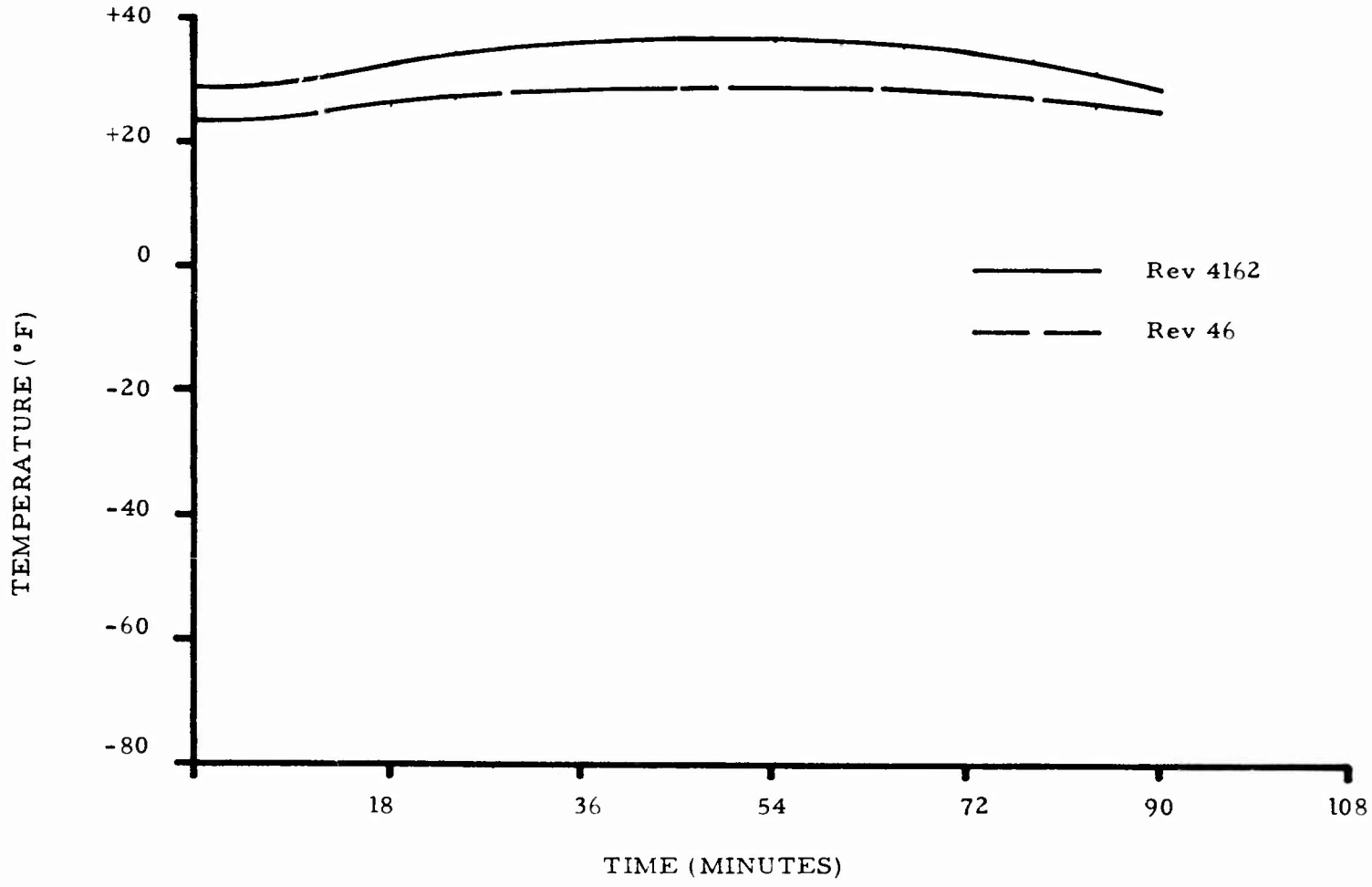

Figure 27. Sensor Temperature vs Time for Temperature Reference During Revolutions 46 and 4162

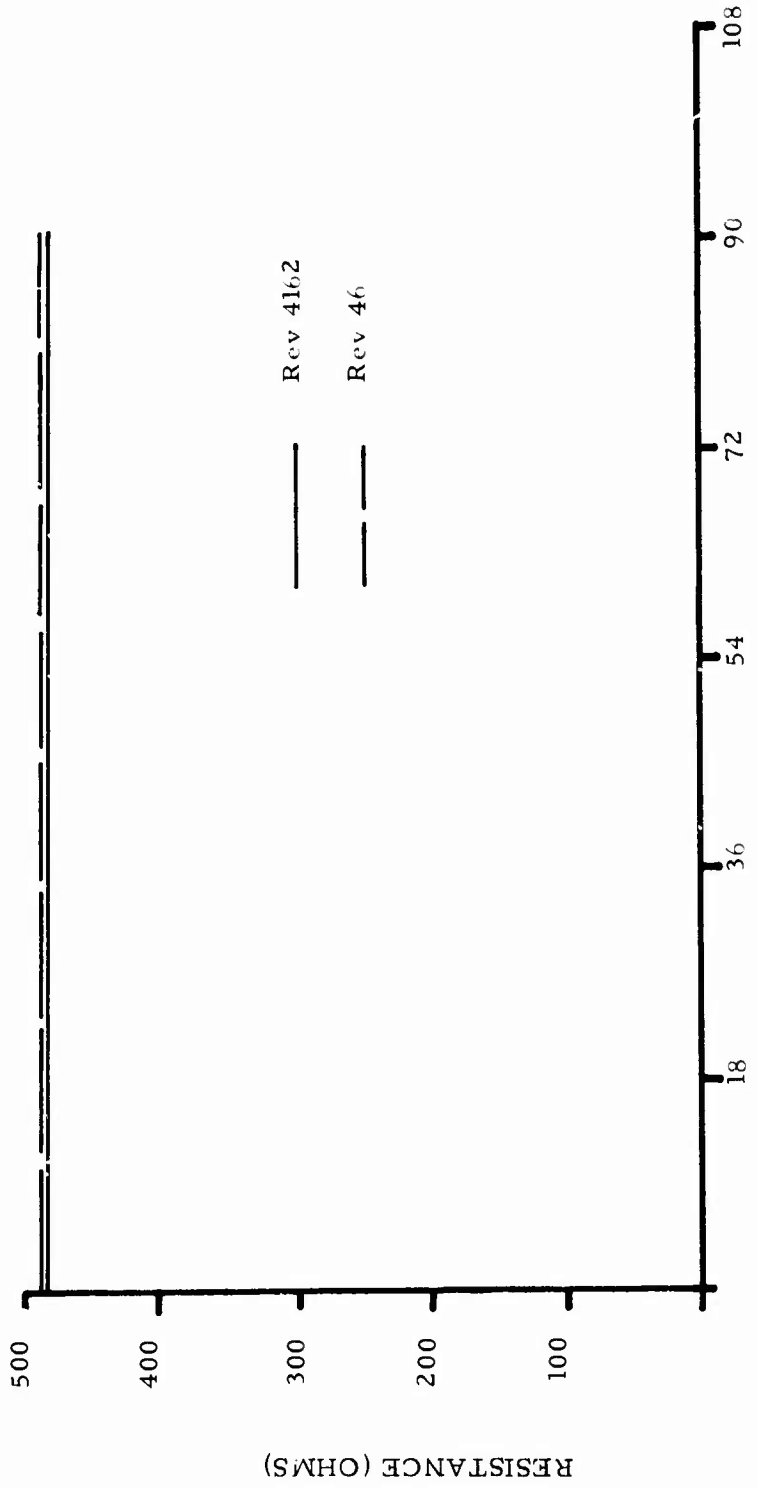

Figure 28. Resistance vs Time for Reference Resistor (499 Ohm)

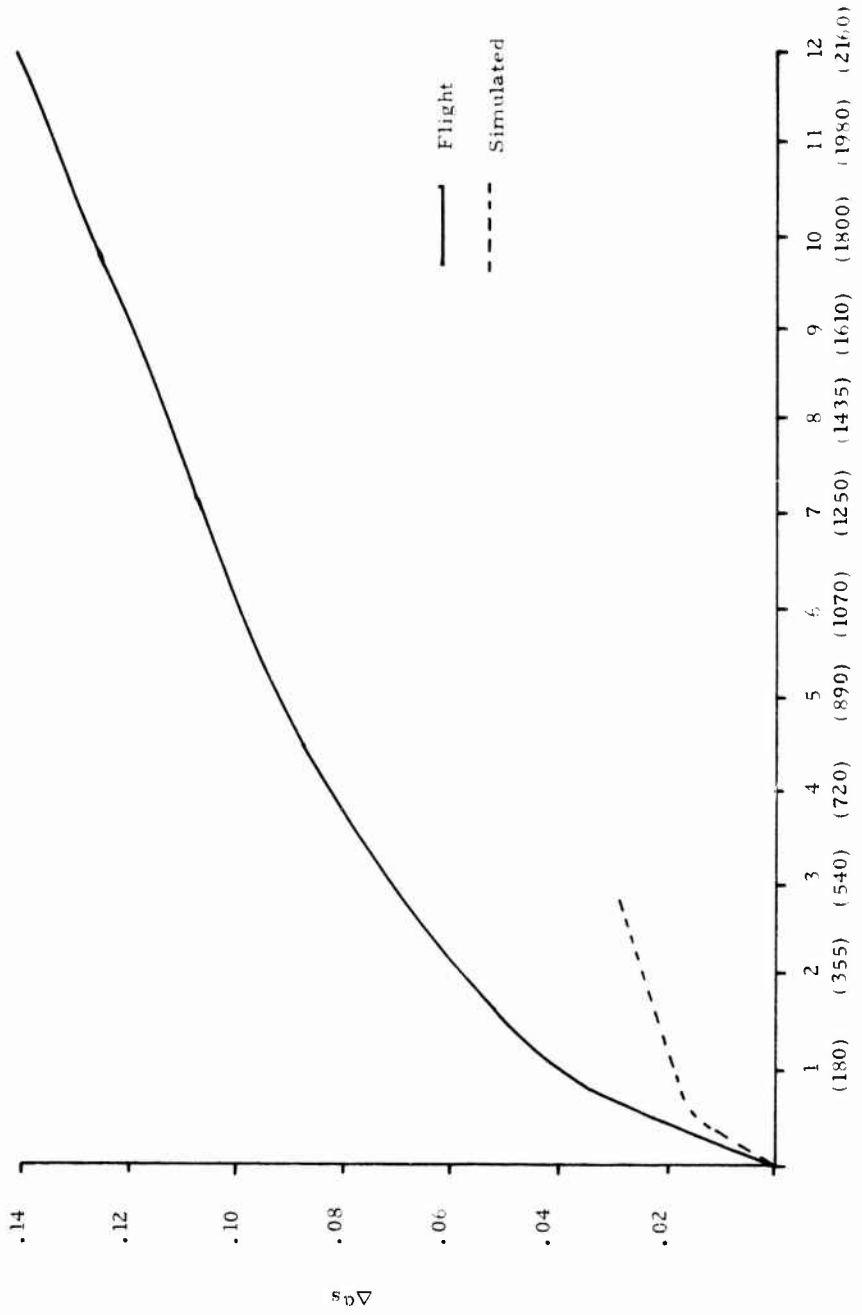

Figure 29. Comparison of Simulated and Flight Data for S-13G

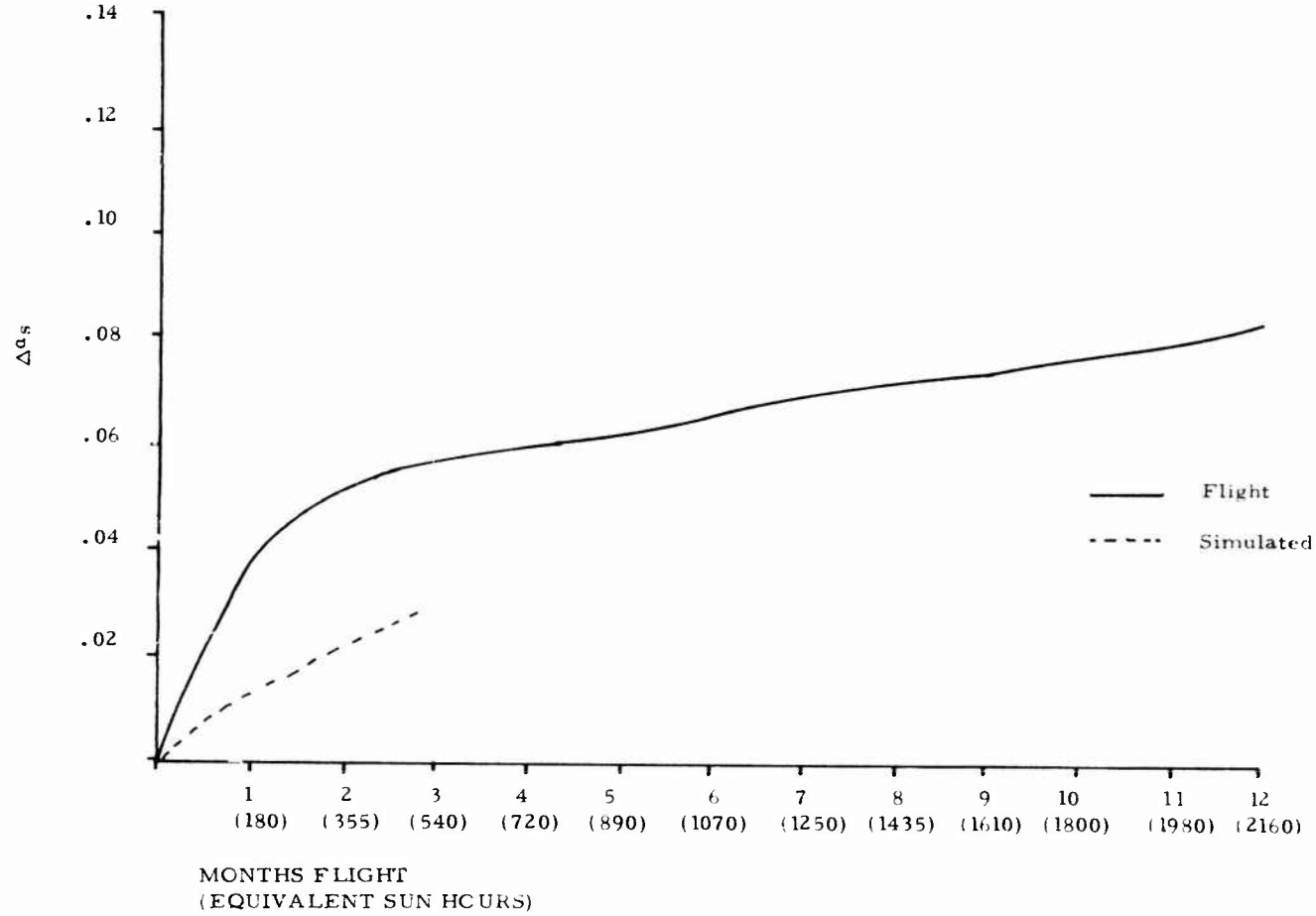

Figure 30. Comparison of Simulated and Flight Data for SiO_2 Fabric

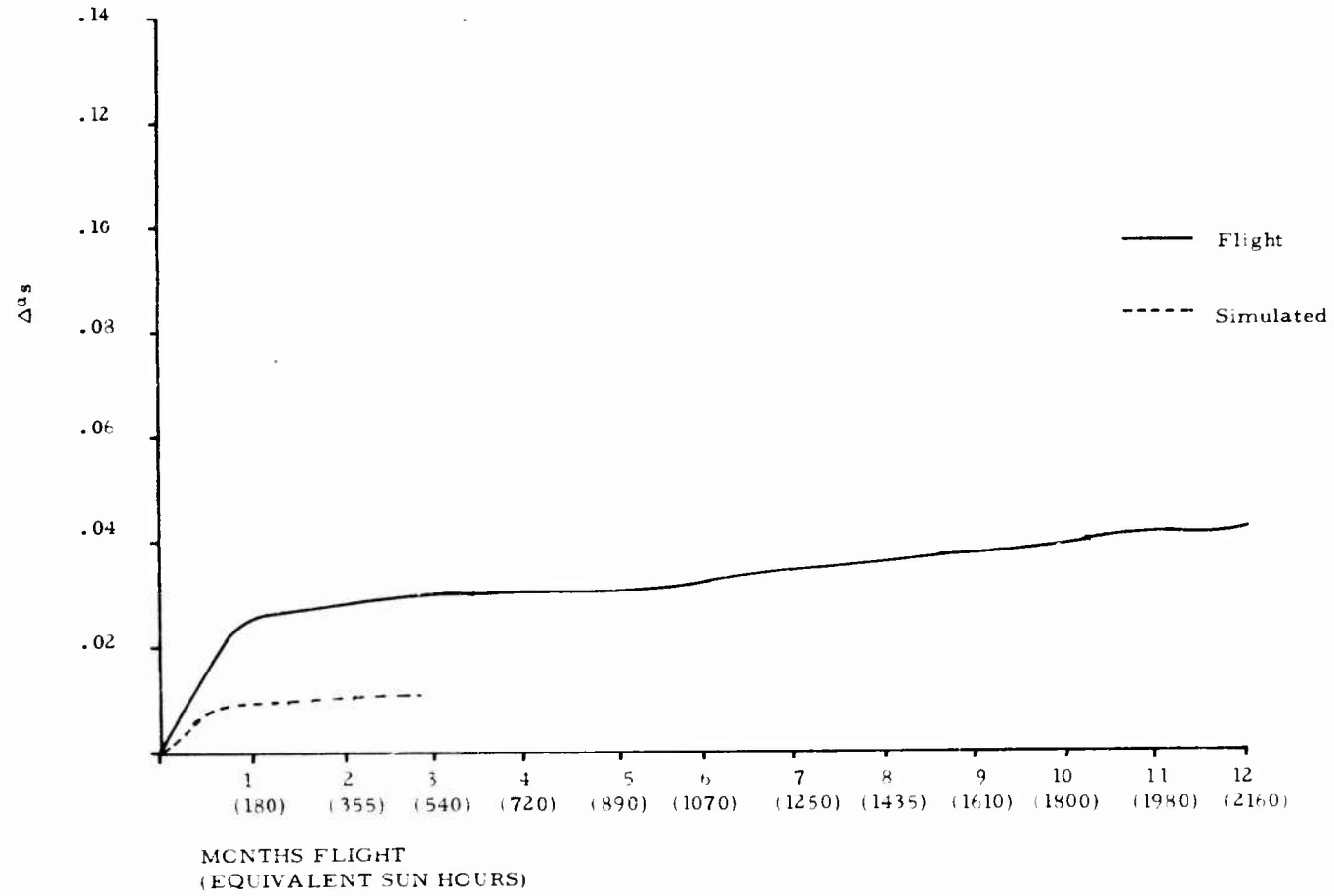

Figure 31. Comparison of Simulated and Flight Data for FEP/A1

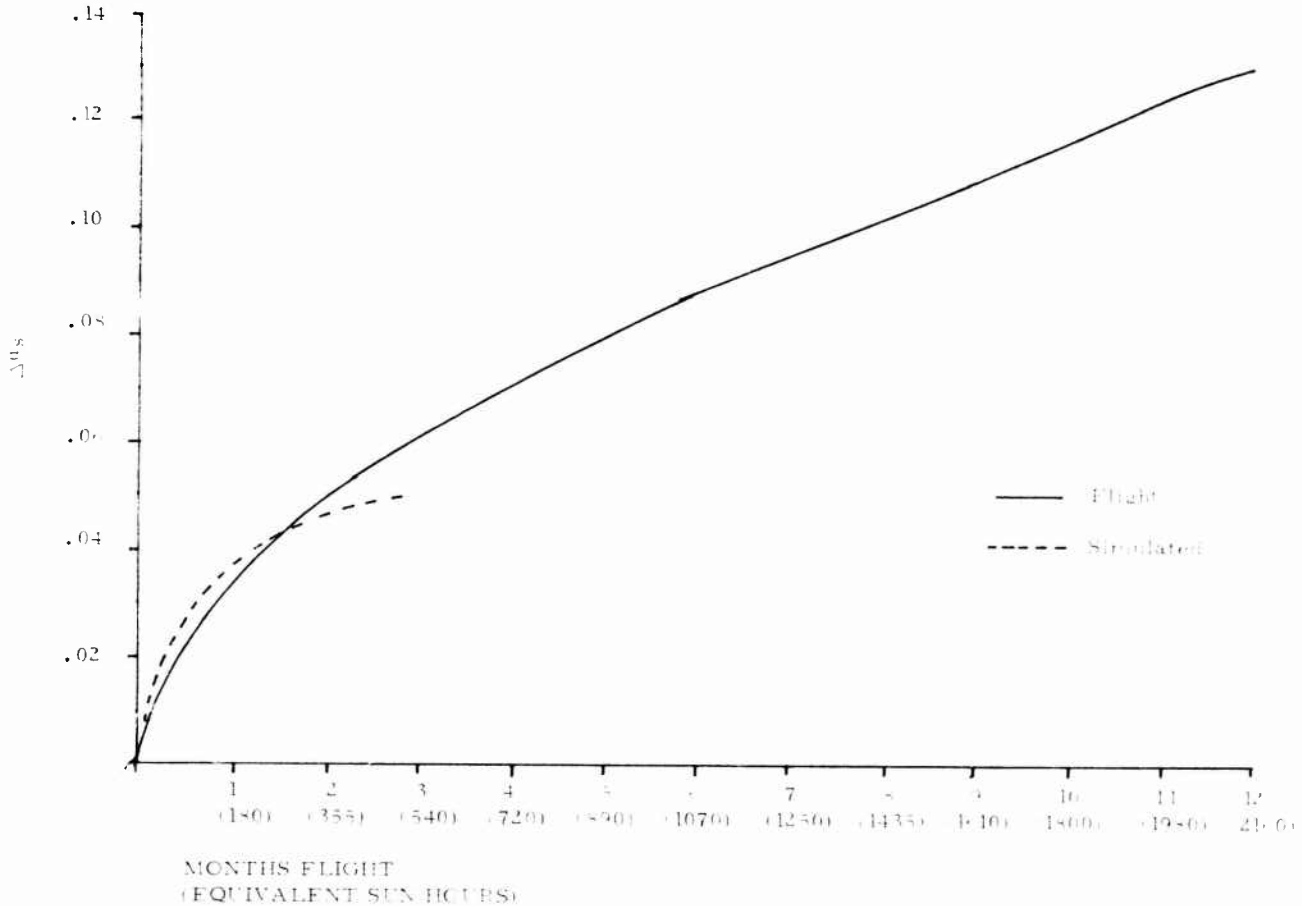

Figure 32. Comparison of Simulated and Flight Data for Zn_2TiO_4/OI650

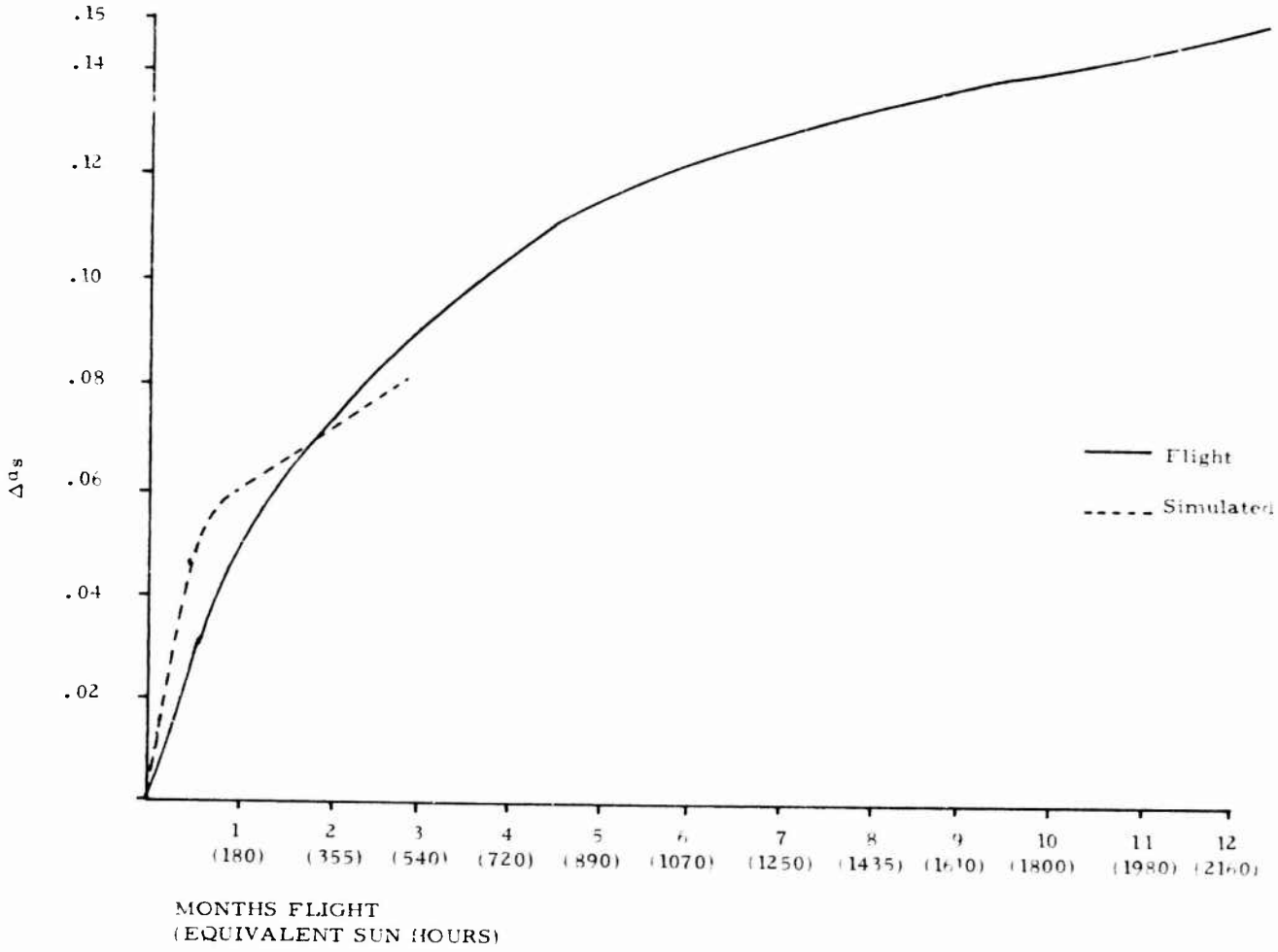

Figure 33. Comparison of Simulated and Flight Data for PV-100

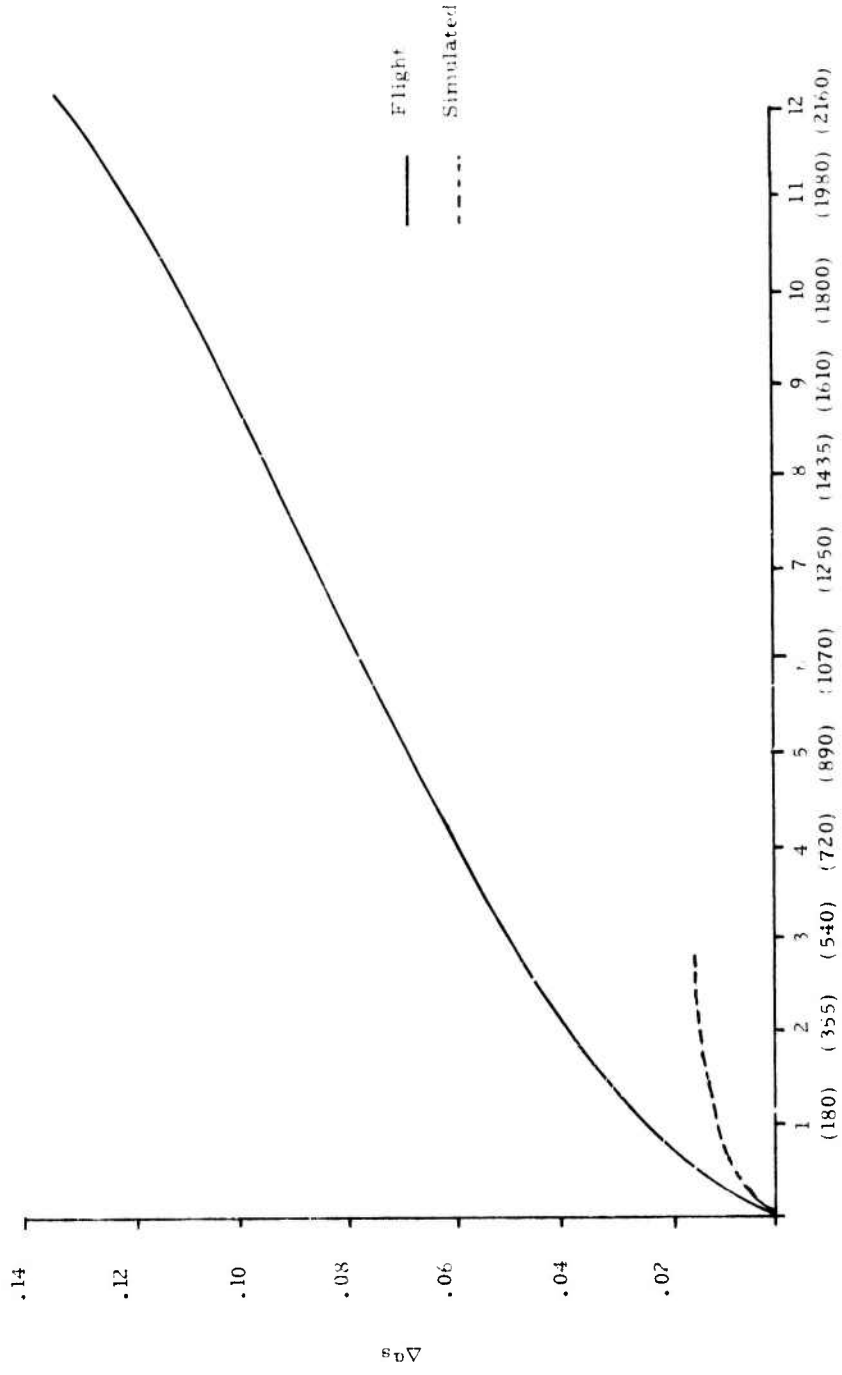

Figure 34. Comparison of Simulated and Flight Data for TiO_2/Silicone

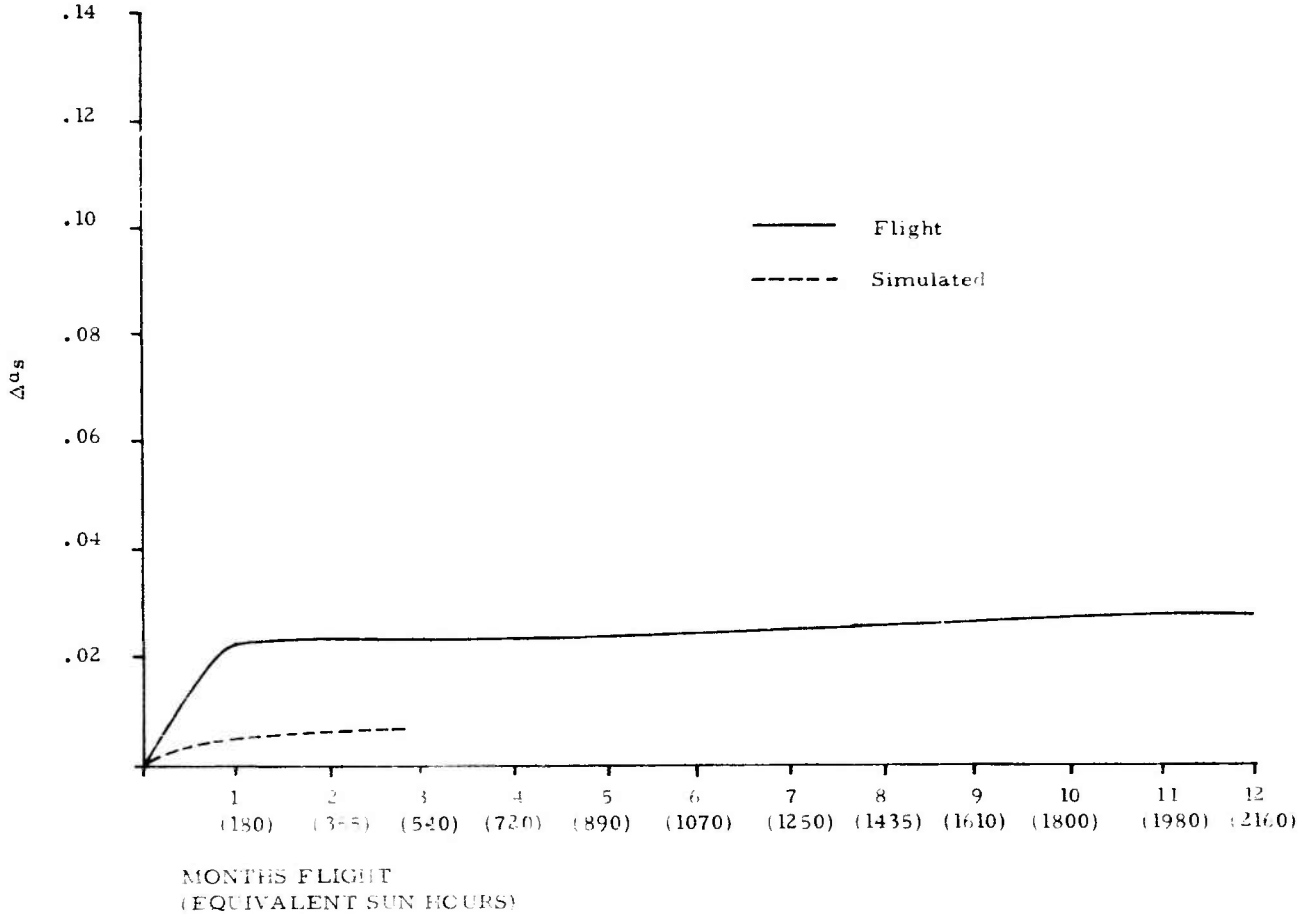

Figure 35. Comparison of Simulated and Flight Data for OSR (0.008)

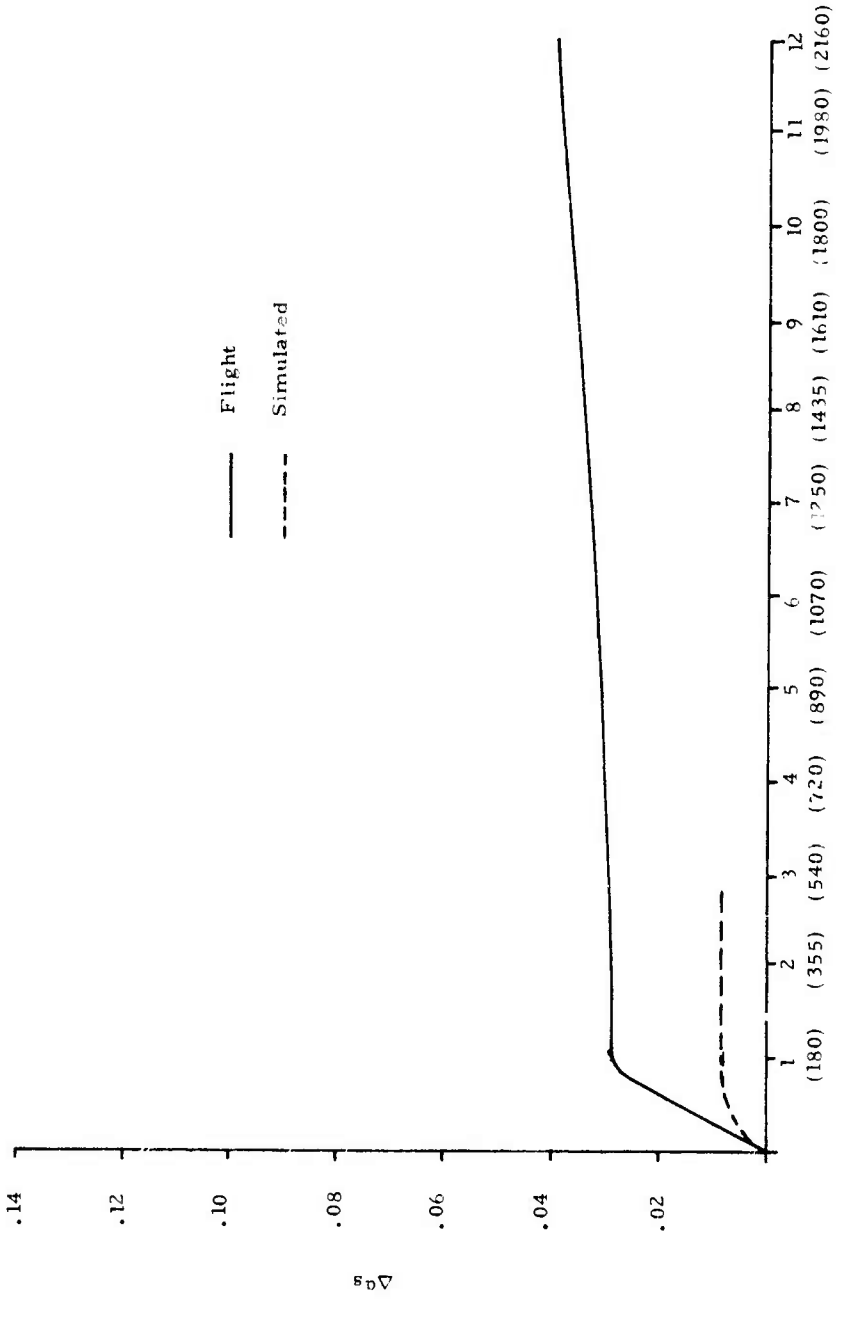

Figure 36. Comparison of Simulated and Flight Data for OSR (0.050)

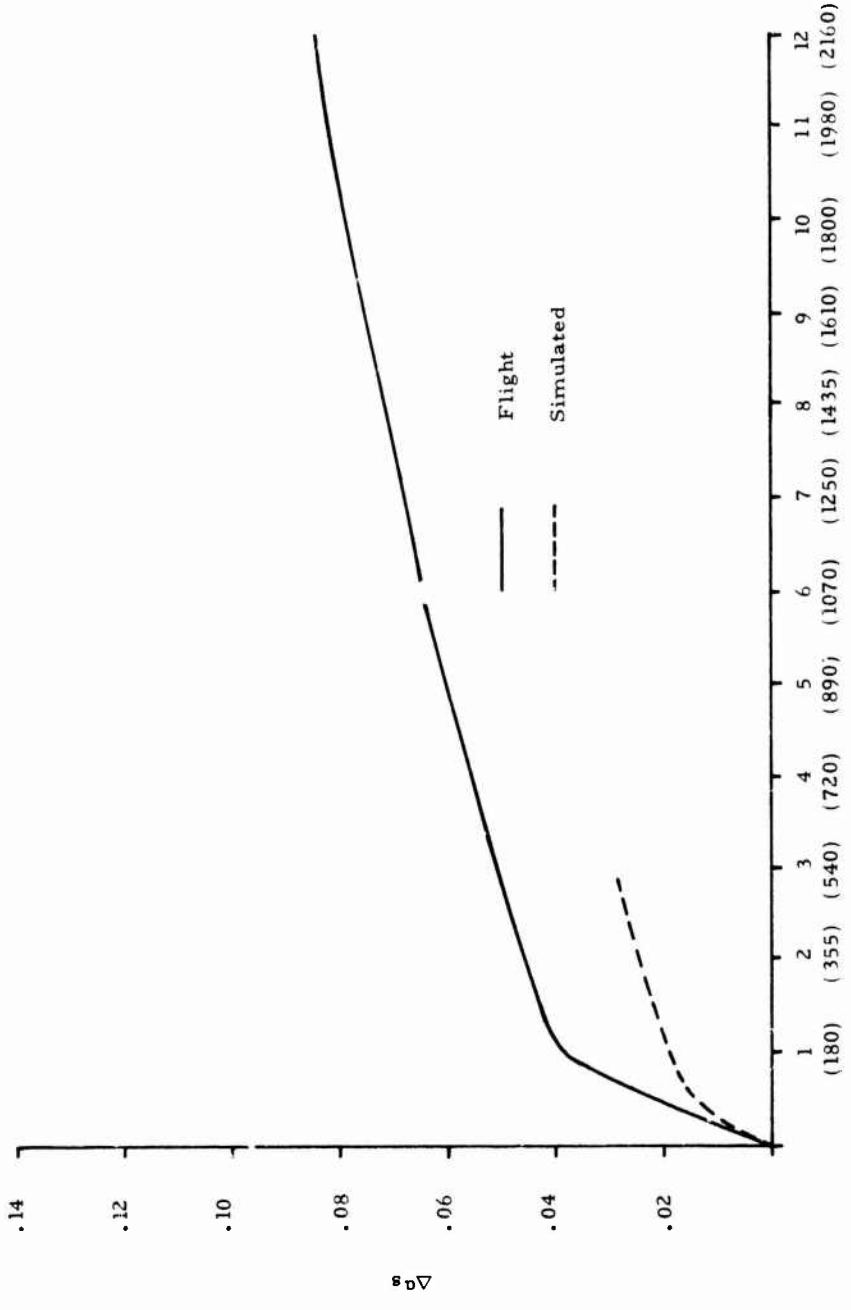

Figure 37. Comparison of Simulated and Flight Data for Eu_2O_3/Silicone

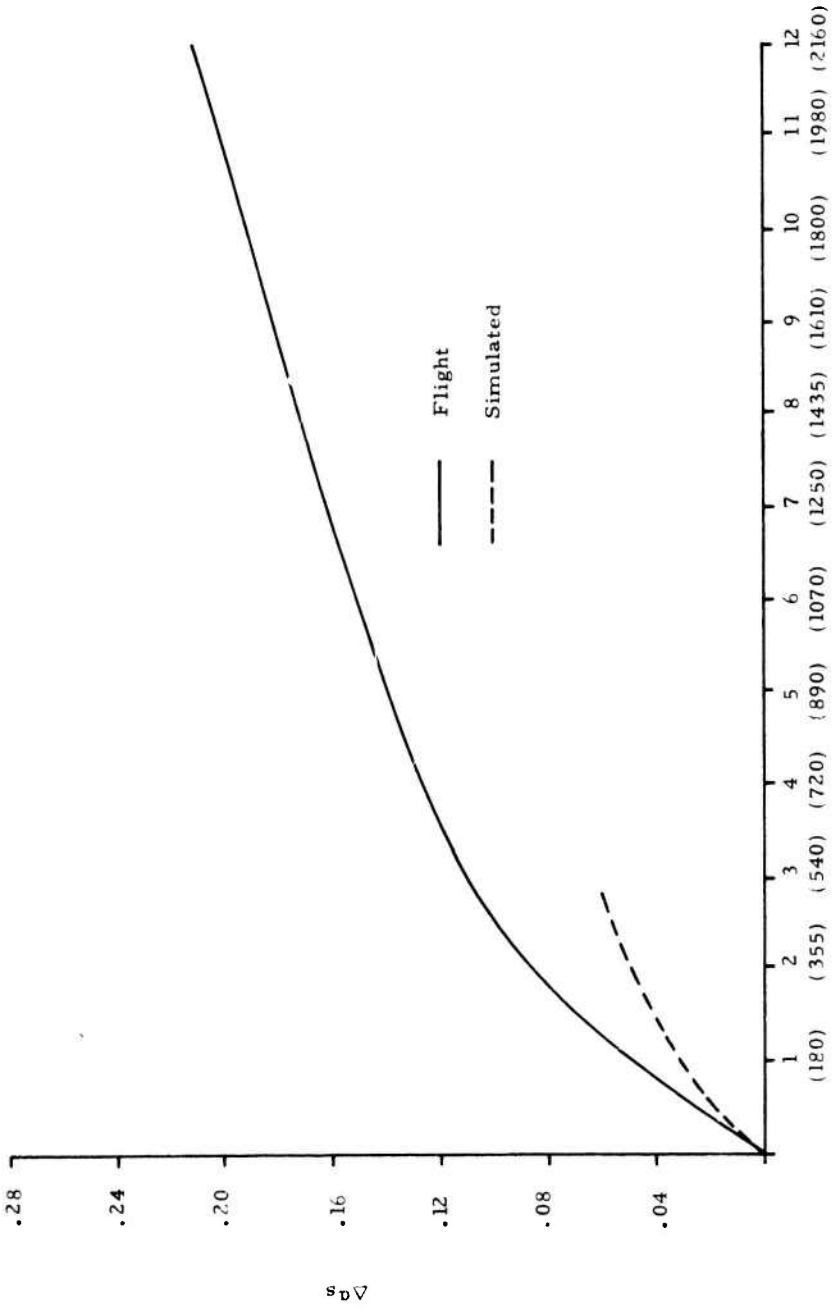

Figure 38. Comparison of Simulated and Flight Data for α-Al_2O_3/Silicone

☆ U. S. GOVERNMENT PRINTING OFFICE: 1975 — 657-650/280